Title No. 115-S11

Punching Shear Strength of Slabs and Influence of Low Reinforcement Ratio

by Susanto Teng, Khatthanam Chanthabouala, Darren T. Y. Lim, and Rhahmadatul Hidayat

Presented in this paper are the punching shear tests of 12 high-strength concrete slabs (f_c' > 100 MPa [14,500 psi]) with various flexural reinforcement ratios from 0.28 to 1.43% and supported on columns having various aspect ratios of 1 x 1, 1 x 3, and 1 x 5. The resulting test data were also used to verify the suitability of the ACI 318 and Eurocode 2 punching shear equations, especially for slabs with low reinforcement ratios.

Other influencing factors such as concrete strength and size effect were also addressed. The authors' new experimental results will be combined with 355 existing published data and together they will be used to evaluate the accuracies and safety of the ACI 318 and Eurocode 2 methods for punching shear, as well as some methods proposed by other researchers. A new general method and a simplified method are also proposed; they are shown to be accurate and reliable.

Keywords: building codes; column aspect ratio; concrete slabs; flexural failure; high-strength concrete; punching shear; reinforcement ratio; shear failure; size effect.

INTRODUCTION

Punching shear failure is one of the critical failure modes that can happen in a flat-plate floor system. Some of the important design parameters that can influence the punching shear strength of concrete slabs include concrete strength, amount of flexural reinforcement, column rectangularity (aspect) ratio, and size effect.

One of the parameters that has not been sufficiently investigated in the past is the influence of the amount of flexural reinforcement ratio ρ ($=A_s/bd$), especially the low reinforcement ratio. Floor slabs with low reinforcement ratios are frequently encountered in the design of flat-plate floors for lightly loaded buildings, such as apartment and condominium buildings or office buildings. The typical values of the required flexural reinforcement ratios ρ ($=A_s/bd$) in the column strips of the flat-plate floors in those buildings can vary from approximately 0.6 to 0.8%. It has been known that when a floor slab is provided with a low flexural reinforcement ratio (ρ of approximately 0.7% or less), the slab may not be able to attain its punching shear capacity as calculated using the ACI 318-14[1] equations for punching shear. That is because it may fail at a lower load due to widespread yielding of the flexural reinforcement. Essentially, that is a flexural failure under punching shear load. A further increase in loading beyond the peak load will only increase slab rotation or deflection before it reaches the final failure in what looks like a punching failure—albeit a ductile punching failure. So far, the ACI 318 or the Eurocode 2[2] (EC2) equations for punching shear have not been sufficiently verified for cases of slabs with low reinforcement ratios where flexural failure under punching load may occur ahead of the normal punching shear failure.

One typical way to treat this lightly reinforced slab case in practice is to calculate the punching strength of the slab using the ACI punching shear equations and compare it with the failure load (ultimate shear force) that causes flexural failure of the slab as calculated using the yield line theory. The lower of these two failure loads will be the punching shear capacity of the slab. However, it would be much easier if Code method can treat cases of low reinforcement ratio directly.

To address the issues mentioned previously, the authors present an experimental program involving the testing of 12 high-strength concrete slabs having various flexural reinforcement ratios and various column aspect (rectangularity) ratios subjected to concentric punching loads. The authors have previously tested similar slabs made of normal-strength concrete to investigate the influence of column aspect ratio as well as opening.[3] Those earlier tests will be useful in current research. In addition, the authors' new experimental results will also be combined with 355 existing published data and together they will be used to evaluate the accuracies of the ACI 318-14 and Eurocode 2 methods, as well as the methods proposed by other researchers.[4-6] A new general method and a simplified method are also proposed; they are shown to be accurate and reliable.

RESEARCH SIGNIFICANCE

A new way to treat punching shear strength of concrete slabs is presented herein. The influence of low flexural reinforcement ratio is considered rationally, resulting in two proposed methods: a proposed general method and a proposed simplified method. The new proposed methods were verified for accuracy using the authors' new experiment, which is also presented in this paper, as well as 355 slab data from literature. The proposed methods were also thoroughly compared with existing methods proposed by other researchers as well as with the methods of ACI 318 and Eurocode 2.

EXPERIMENTAL PROGRAM

The slab specimens in this experimental program were designed to cover a low range of reinforcement ratios as well as some of the higher ranges of reinforcement ratios to

ACI Structural Journal, V. 115, No. 1, January 2018.
MS No. S-2016-432, doi: 10.14359/51701089, was received December 8, 2016, and reviewed under Institute publication policies. Pertinent discussion including author's closure, if any, will be published ten months from this journal's date if the discussion is received within four months of the paper's print publication.

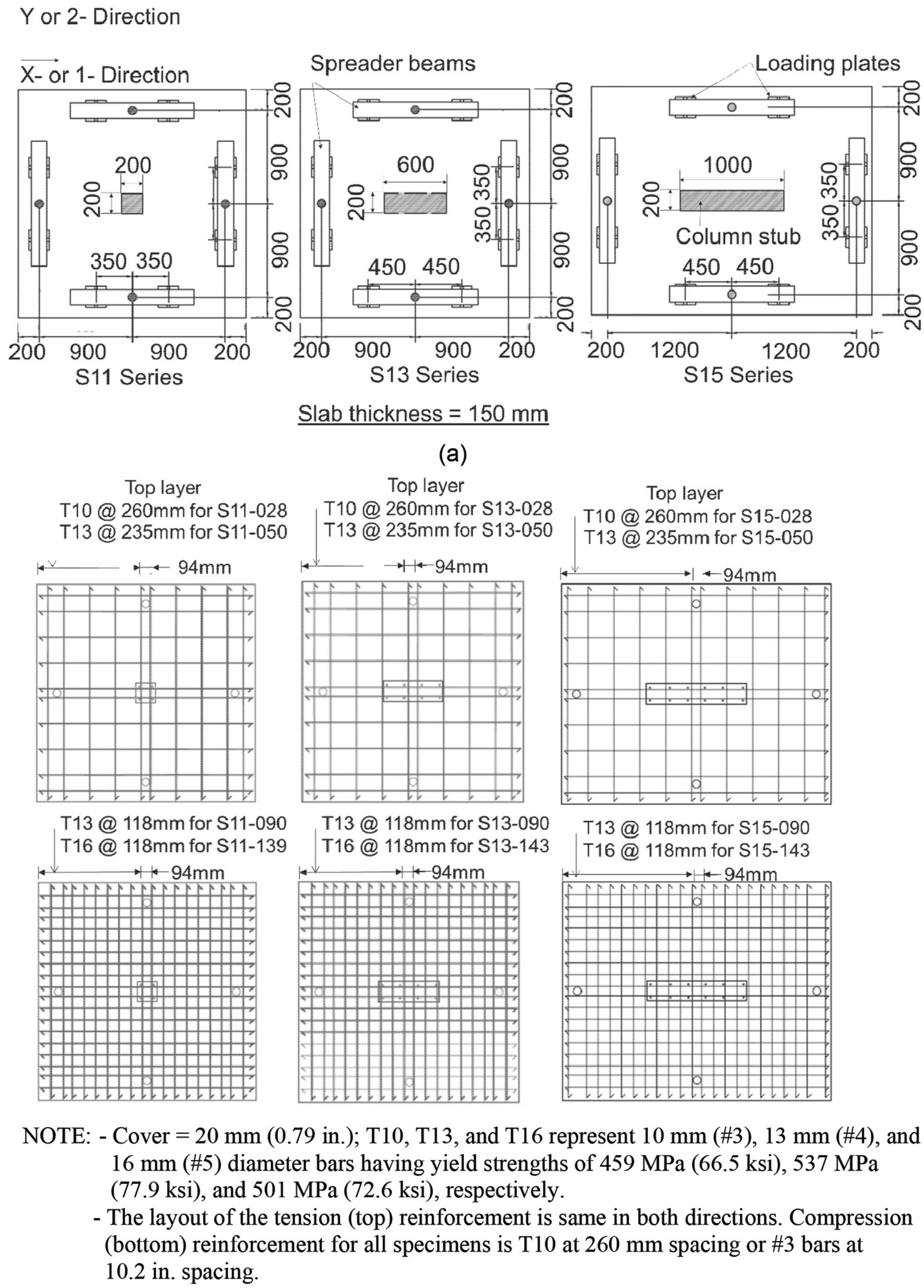

(b)

Fig. 1—(a) General dimensions and loading positions; and (b) reinforcement details.

provide a more complete set of data. The dimensions of the specimens represent an actual model of the column zone of flat-plate slabs having column-to-column spans of approximately 5.0 to 6.0 m (16.4 to 19.7 ft).

Specimen details and material properties

The 12 slab specimens tested in this experiment were categorized into three main groups: S11 series, S13 series, and S15 series to represent their corresponding column aspect ratios of 1 x 1, 1 x 3, and 1 x 5, respectively. Figure 1(a) shows the general dimensions of the slab specimens and their loading positions while Fig. 1(b) shows the reinforcement details of the 12 slab specimens. Table 1 summarizes important properties of the specimens. The overall dimensions (L_1 x L_2 x h) of the specimens were 2.2 x 2.2 x 0.15 m (87 x 87 x 5.9 in.) for the S11 and S13 series, and 2.7 x 2.2 x 0.15 m (106 x 87 x 5.9 in.) for the S15 series. The cross-sectional dimensions of the column stubs were 200 x 200 mm (7.9 x 7.9 in.) for the S11 series, 600 x 200 mm (23.7 x 7.9 in.) for the S13 series, and 1000 x 200 mm (39.5 x 7.9 in.) for the S15 series. The height of the column stub was 200 mm (7.9 in.) for all specimens. In addition to the main top reinforcement, all the specimens were provided with bottom reinforcement in the form of 10 mm (3/8 in.) diameter bars that were distributed at 260 mm (10.2 in.) spacing, denoted as T10@260 mm (No. 3@10.2 in.) in Fig. 1(b).

Table 1—Properties of slab specimens

	No.	Slab ID	Dimensions, m (in.)	Column size, m (in.)	*d*, mm (in.)	f_c', MPa (ksi)	f_y, MPa (ksi)	ρ, %	Top reinforcement bar size @ spacing, mm (in.)
(1)	(2)	(3)	(4)	(5)	(6)	(7)	(8)	(9)	(10)
S11 Series	1	S11-028	2.2 x 2.2 x 0.15 (87 x 87 x 5.9)	0.2 x 0.2 (7.9 x 7.9)	120 (4.7)	112.0 (16.2)	459 (66.5)	0.28	T10@ 260 (No. 3 @ 10.2)
	2	S11-050			117 (4.6)		537 (77.9)	0.50	T13@ 235 (No. 4 @ 9.2)
	3	S11-090			117 (4.6)		537 (77.9)	0.90	T13@ 118 (No. 4 @ 4.6)
	4	S11-139			114 (4.5)		501 (72.6)	1.39	T16@ 118 (No. 5 @ 4.6)
S13 Series	5	S13-028	2.2 x 2.2 x 0.15 (87 x 87 x 5.9)	0.2 x 0.6 (7.9 x 23.7)	120 (4.7)	114.0 (16.5)	459 (66.5)	0.28	T10@ 260 (No. 3 @ 10.2)
	6	S13-050			117 (4.6)		537 (77.9)	0.50	T13@ 235 (No. 4 @ 9.2)
	7	S13-090			117 (4.6)		537 (77.9)	0.90	T13@ 118 (No. 4 @ 4.6)
	8	S13-143			114 (4.5)		501 (72.6)	1.43	T16@ 118 (No. 5 @ 4.6)
S15 Series	9	S15-028	2.7 x 2.2 x 0.15 (106.4 x 87 x 5.9)	0.2 x 1.0 (7.9 x 39.5)	120 (4.7)	97.0 (14)	459 (66.5)	0.28	T10@ 260 (No. 3 @ 10.2)
	10	S15-050			117 (4.6)		537 (77.9)	0.50	T13@ 235 (No. 4 @ 9.2)
	11	S15-090			117 (4.6)		537 (77.9)	0.90	T13@ 118 (No. 4 @ 4.6)
	12	S15-143			114 (4.5)		501 (72.6)	1.43	T16@ 118 (No. 5 @ 4.6)

Notes: Concrete cover = 20 mm (0.8 in.); maximum aggregate size = 20 mm (0.8 in.); same reinforcement is provided in both directions; T10 @ 260 mm = 10 mm bars at 260 mm spacing or No. 3 bar (3/8 in.) at 10.2 in. spacing; *d* is average effective depth f_c' is cylinder compressive strength of concrete; f_y is yield strength of flexural reinforcement; ρ is average reinforcement ratio $(\rho_x + \rho_y)/2$; $\rho_x = 100A_{sx}/(L_x \times d_x)$.

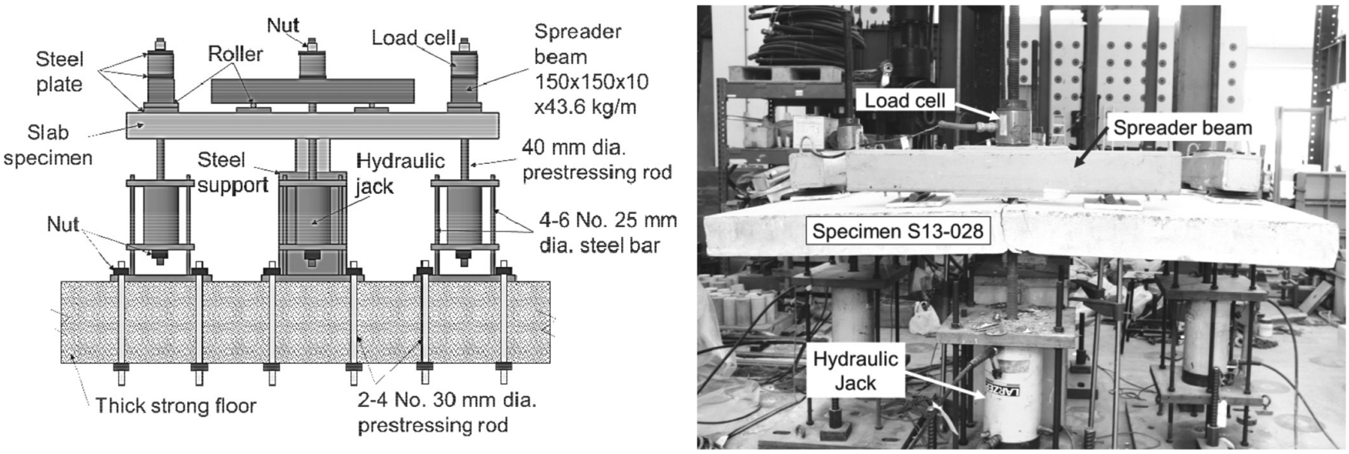

(a) (b)

Fig. 2—(a) Typical test setup; and (b) Specimen S13-028 during testing.

The specimen notation represents the main properties of the slab specimens. For example, Specimen S13-143 indicates a slab specimen with a column aspect ratio of 1 x 3 (β = 3) and flexural reinforcement ratio ρ of 1.43%.

The strengths of the concrete used in all the specimens were approximately 100 MPa (14,500 psi) (refer to Column 7 of Table 1). The maximum aggregate size is 20 mm (0.8 in.). Some of the advantages of using high-strength concrete compared to normal-strength concrete include an increase in cracking load of the slab and a reduction in deflection at service load level due to higher tensile strength and higher elastic modulus of higher-strength concrete. Higher concrete strength also leads to higher durability in adverse environments.

Instrumentation and loading procedure

A typical test setup and a photograph of a slab during testing are shown in Fig. 2. Each specimen was placed on a steel support block and then vertically loaded downward through four hydraulic jacks that were secured onto the laboratory strong floor. Each hydraulic jack would apply the loading by pulling down the steel rod, which transferred the pulldown force to the spreader beams and then onto the loading plates (points) on the slab. The actual positions of the spreader beams and loading points (Fig. 1(a)) were determined using a finite element software such that the distributions of stresses near the column zone were close to those stress distributions in the same slab when loaded under uniform loading.

Strain gauges were installed on some of the top reinforcing bars in both directions and linear variable differential transformers (LVDTs) were placed below the slab along the column center lines to measure vertical deflections at every load increment.

Each specimen was loaded at 20 kN (4.5 kip) load increment or approximately 5 kN (1.12 kip) increment for each jack. At every load increment, readings of vertical displacements from LVDTs and steel strains were recorded all the

Table 2—Comparison of design methods with current test results

								V_{exp}/V_{calc}					
Slab ID	c_2 x c_1, mm (in.)	d, mm (in.)	ρ, %	V_{exp}*, kN (kip)	Failure mode†	ρ_{fs}‡, %	ρ/ρ_{fs}§, (4)/(7)	ACI 318-14	Eurocode 2	Peiris-Ghali	CSCT	Proposed General Method	Proposed Simplified Method
(1)	(2)	(3)	(4)	(5)	(6)	(7)	(8)	(9)	(10)	(11)	(12)	(13)	(14)
S11-028	200 x 200 (7.9 x 7.9)	120 (4.7)	0.28	280 (62.9)	F	0.96	0.29 (F)	0.65	0.96	1.92	1.12	1.19	1.13
S11-050		117 (4.6)	0.50	394 (88.6)	F	0.98	0.51 (F)	0.95	1.16	1.58	1.21	1.29	1.22
S11-090		117 (4.6)	0.90	440 (98.9)	P	0.78	1.16 (P)	1.06	1.06	1.06	0.99	1.06	1.06
S11-139		114 (4.5)	1.39	454 (102.1)	P	0.88	1.58 (P)	1.14	0.99	1.14	0.89	0.98	0.98
S13-028	200 x 600 (7.9 x 23.7)	120 (4.7)	0.28	308 (69.2)	F	0.98	0.27 (F)	0.53	0.79	2.18	0.99	1.07	1.01
S13-050		117 (4.6)	0.50	418 (94.0)	F	0.80	0.63 (F)	0.74	0.91	1.44	0.97	1.06	1.04
S13-090		117 (4.6)	0.90	558 (125.4)	P	0.80	1.13 (P)	0.99	1.00	1.08	0.96	1.08	1.08
S13-143		114 (4.5)	1.43	718 (161.4)	P	0.91	1.57 (P)	1.32	1.14	1.32	1.05	1.23	1.23
S15-028	200 x 1000 (7.9 x 39.5)	120 (4.7)	0.28	322 (74.4)	F	1.07	0.25 (F)	0.49	0.68	2.42	0.97	1.04	0.97
S15-050		117 (4.6)	0.50	458 (103.0)	F	0.85	0.58 (F)	0.70	0.79	1.59	0.95	1.04	1.00
S15-090		117 (4.6)	0.90	658 (147.9)	P	0.85	1.06 (P)	1.00	0.93	1.28	1.00	1.12	1.12
S15-143		114 (4.5)	1.43	776 (174.4)	P	0.97	1.47 (P)	1.22	0.98	1.22	0.99	1.17	1.17
							Minimum	0.49	0.68	1.06	0.89	0.98	0.97
							Maximum	1.32	1.16	2.42	1.21	1.29	1.23
							Average	0.90	0.95	1.52	1.01	1.11	1.08
							Coefficient of variation	0.30	0.15	0.29	0.084	0.082	0.083

*V_{exp} is total failure load, including weight of specimen outside distance d from column face and weight of test equipment on top of specimen.

†Observed failure mode: F is flexural failure; P is punching failure.

‡ρ_{fs} is proposed limiting reinforcement ratio, calculated using Eq. (12a), ρ_{fs} is taken to be 0.007 for proposed Simplified Method as shown by Eq. (12b).

§For $\rho/\rho_{fs} > 1.0$, the predicted failure mode is punching; for $\rho/\rho_{fs} \leq 1.0$, the predicted failure mode is flexure. ρ_{fs} in Column (7) is for proposed Standard Method and calculated using Eq. (12a).

way to failure. Crack widths were measured by using a crack detector until near failure.

TEST RESULTS AND DISCUSSIONS

Failure loads and crack patterns

The failure loads V_{exp} of the 12 specimens are summarized in Table 2. Each failure load includes the self-weight of the slab outside the perimeter measured at d away from a column face and the weight of test equipment placed on top of the slab. Those slabs that failed abruptly with a sudden drop in their load-deflection curves are indicated to have failed in punching mode (P). Those slabs that failed in a more ductile manner or with widespread yielding of reinforcement prior to punching failure are indicated to have failed in flexural (F) mode. All the slabs finally failed in what appears to be punching failure, even though the slabs might have failed earlier in flexural mode.

Figure 3 shows the photographs of the crack patterns at the failure of the S11-series. The crack patterns of the other eight slabs are shown in Fig. 4. Figure 3 shows fairly clearly that slabs with low reinforcement ratios would have different crack patterns at failure compared to slabs with high reinforcement ratios. Typical crack patterns of slabs failing in normal punching can be seen in Fig. 3(c) and (d), which show Specimens S11-090 and S11-139, respectively. The crack pattern in each of these cases comprises a set of closely spaced radial cracks or circular-fan-type cracks with

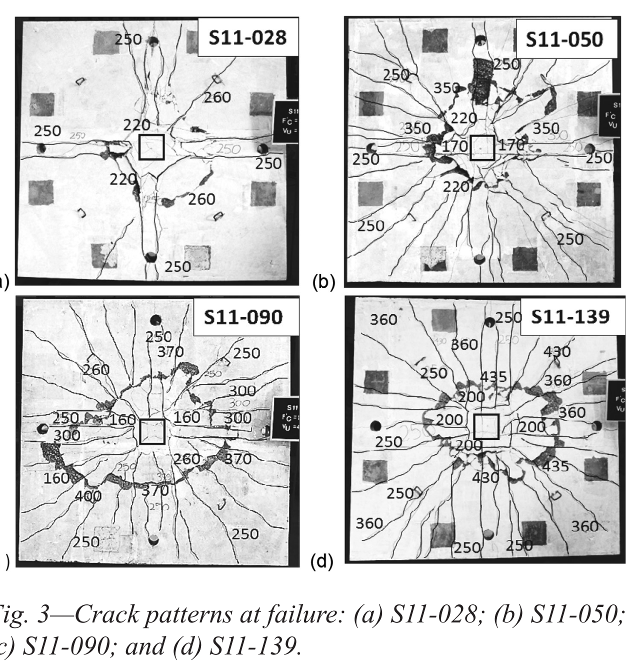

Fig. 3—Crack patterns at failure: (a) S11-028; (b) S11-050; (c) S11-090; and (d) S11-139.

the final circumferential crack that comes to the surface from the internal inclined shear cracks.

If the reinforcement ratio is low, however, the circular-fan-type of crack pattern may not form. Figure 3(a) shows the crack pattern of Slab S11-028; it can be seen that the crack pattern forms straight-line cracks nearly parallel

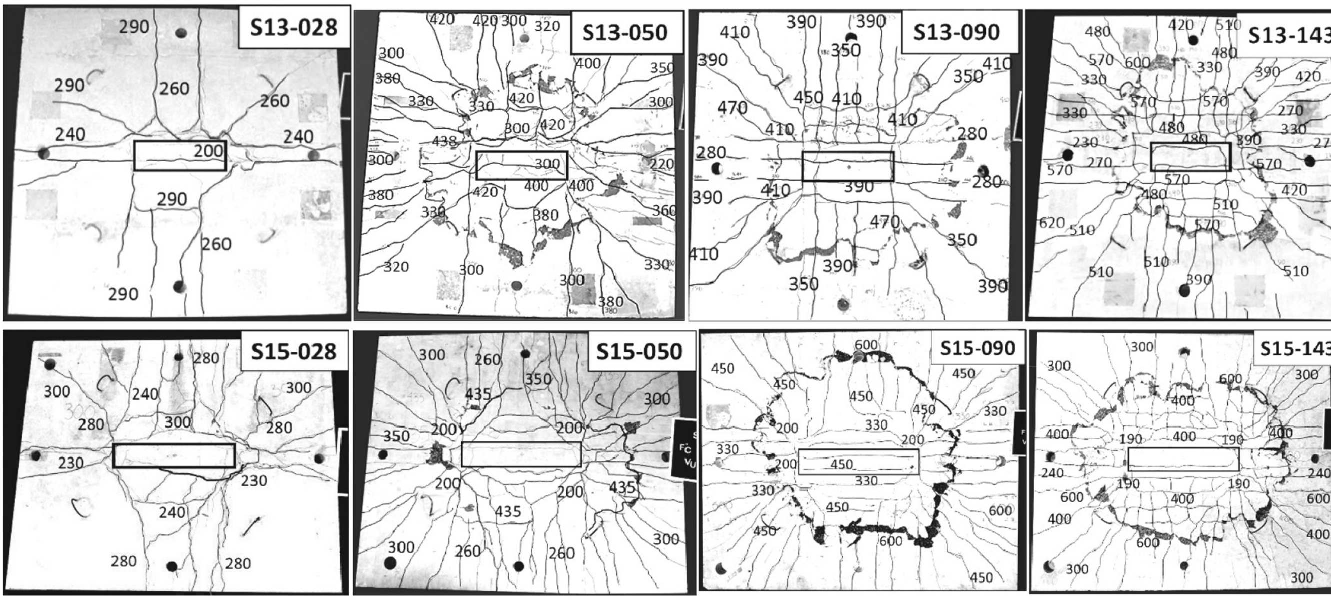

Fig. 4—Crack patterns of S13 and S15 series at failure.

to column lines in both directions with perhaps one diagonal crack from the column corner toward a corner of the slab. The parallel line crack pattern shows that widespread yielding of the reinforcement has occurred. In the end, the final failure of the slab would still be a punching failure with the final circumferential crack occurring very close to the column. The failure load is at a load no greater than the load that caused earlier yielding of the flexural reinforcement. Similar behavior and crack patterns can also be seen in other specimens with low reinforcement ratios such as S13-028 (ρ = 0.28%) and S15-028 (ρ = 0.28%), as shown in Fig. 4.

Deflections

The load-deflection curves of the 12 specimens are shown in Fig. 5. Each curve shows the average of four deflection points located 100 mm (3.9 in.) from the slab edges. Before cracking, the relationship between the load and deflection is linear. After the first circumferential crack formed, the slope of the load-deflection curve would change slightly. Upon further loading, the change of slope becomes increasingly more significant as the flexural stiffness of the slab drops further due to more cracking or widening of cracks. As expected, the flexural stiffness of the slab with a higher reinforcement ratio will degrade less after cracking—that is, its load-deflection curves have steeper slopes compared to slabs with low reinforcement ratios.

Figure 5 also shows that slabs with lower reinforcement ratios are more ductile than slabs with higher reinforcement ratios. Upon reaching the maximum load, any further load increment to Specimen S11-028, S13-028, and S15-028 (very low reinforcement ratios) produces no additional increase in resistance, but their deformations continue to increase until the final failure at the end. The slabs with the highest reinforcement ratio (S11-139, S13-143, and S15-143) are the most brittle. Nevertheless, the slabs with higher reinforcement ratios also have higher failure loads. However, the influence of reinforcement ratio on punching shear strength is neglected in the ACI 318-14.[1]

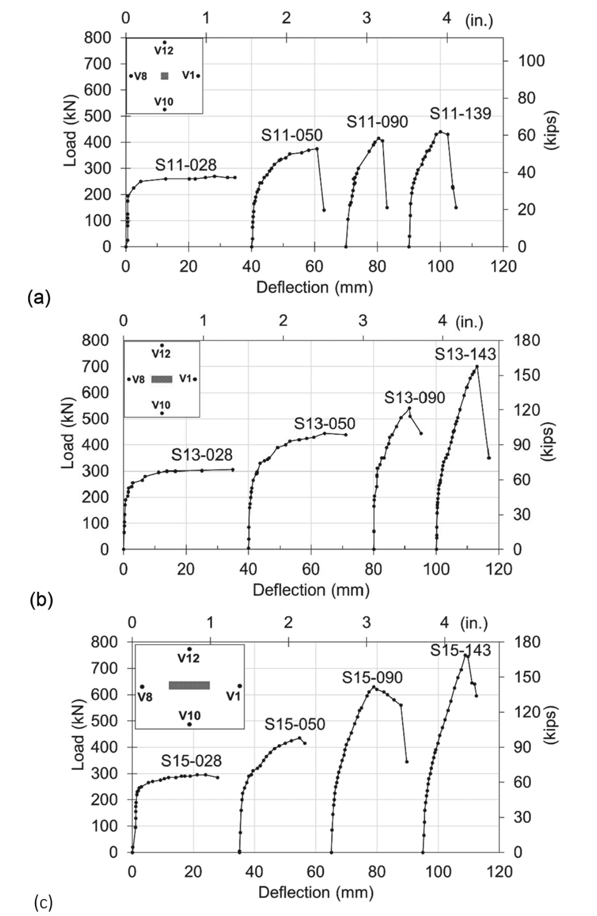

Note: Deflection is the average of four deflections at V1,V8,V10 and V12

Fig. 5—Load-deflection curves of 12 slabs: (a) S11-series; (b) S13-series; (c) S15-series.

Strains in flexural reinforcements

Figure 6 shows the summary of steel strain distributions at the ultimate load stage in the S11-series, S13-series, and S15-series. From Fig. 6, it can be seen that in slabs with higher reinforcement ratios ($\rho \geq 0.9\%$ or Sxy-090 and

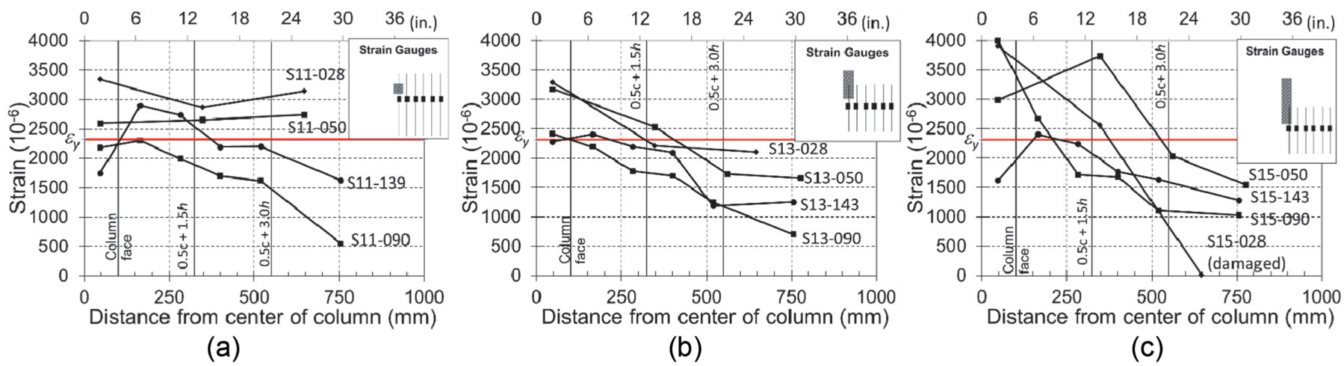

Fig. 6—Steel strains in several reinforcing bars near columns at failure loads for: (a) S11 series slabs; (b) S13 series slabs; and (c) S15 series slabs.

Sxy-143), most of the steel strains drop considerably at locations beyond 1.5h away from the column face. In slabs with lower reinforcement ratios ($\rho \leq 0.5\%$ or Sxy-028 and Sxy-050), the initial failure mode is flexure, and most of the steel strains can remain high or greater than the yield strain even at locations near the edge of the slabs. Thus, in slabs that fail in pure punching, the steel strains reach the yield strain only near the column.

The consequence of the aforementioned behavior is that the reinforcement that should be considered effective for resisting punching load are those within approximately 1.5h from the column faces or within a width of $c_2 + 3h$ for an interior column.

DESIGN CODES AND EXISTING DESIGN METHODS

In this section and the next section, the ACI 318, Eurocode 2 methods, and some existing design methods proposed by researchers are discussed briefly.

ACI 318-14[1]

According to ACI 318-14,[1] the punching shear strength V_c of slabs without shear reinforcement can be determined from the lowest of the following expressions

$$V_c = \frac{1}{12}(2 + 4/\beta)\sqrt{f_c'}b_o d \quad \text{(SI units)}$$
$$V_c = (2 + 4/\beta)\sqrt{f_c'}b_o d \quad \text{(U.S. units)} \tag{1}$$

$$V_c = \frac{1}{12}(\alpha_s d/b_o + 2)\sqrt{f_c'}b_o d \quad \text{(SI units)}$$
$$V_c = (\alpha_s d/b_o + 2)\sqrt{f_c'}b_o d \quad \text{(U.S. units)} \tag{2}$$

$$V_c = \frac{1}{3}\sqrt{f_c'}b_o d \quad \text{(SI units)}$$
$$V_c = 4\sqrt{f_c'}b_o d \quad \text{(U.S. units)} \tag{3}$$

where β is the ratio of long to short sides of the column; α_s is taken to be 40, 30, and 20 for interior, edge, and corner columns, respectively; and b_o is the length of the critical perimeter located at 0.5d away from the column face. For a circular column, the critical section can also be defined by assuming a square column of equivalent area. The influence of flexural reinforcement and size effect are neglected in the ACI Code equations. ACI 318-14[1] does not limit the maximum concrete strength f_c' but the value of $\sqrt{f_c'}$ used to calculate shear strength is limited to 100 psi (8.3 MPa).

Eurocode 2[2]

According to the Eurocode 2,[2] the punching shear resistance $V_{Rd,c}$ of a slab without shear reinforcement is given in Eq. (4)

$$V_{Rd,c} = 0.18k(100\rho f_c')^{1/3}u_1 d \quad \text{(SI units)}$$
$$V_{Rd,c} = 5k(100\rho f_c')^{1/3}u_1 d \quad \text{(U.S. units)} \tag{4}$$

where k is the size effect coefficient, $= 1 + \sqrt{200/d} \leq 2.0$ (SI units) or $= 1 + \sqrt{8/d} \leq 2.0$ (U.S. units). The ρ is the average flexural reinforcement ratio ($\rho = \sqrt{\rho_x \rho_y} \leq 0.02$). The critical shear perimeter u_1 is located at a distance 2d away from the column faces and it has round corners. Eurocode 2 neglects the effect of column rectangularity in symmetrically loaded slabs.

Existing design methods

Teng et al.[3] investigated the effects of slab openings and column rectangularity in normal-strength reinforced concrete slabs. They proposed a design equation for the punching shear strength V_c, as shown in Eq. (5)

$$V_c = 0.6k_{CR}(100\rho f_c')^{1/3}b_o d \quad \text{(SI units)}$$
$$V_c = 16.6k_{CR}(100\rho f_c')^{1/3}b_o d \quad \text{(U.S. units)} \tag{5}$$

where

$$k_{CR} = (b_2/b_1)^{1/4} \leq 1.0 \tag{6}$$

where b_1 and b_2 are the longer and shorter sides of the critical shear perimeter, respectively. The use of b_1 and b_2 in the column rectangularity factor, k_{CR}, rather than c_1 and c_2, is to take into consideration the thickness of the slab in influencing the distribution of stresses around the column. The critical shear perimeter b_o has square corners for both square and circular columns and is located at a distance d/2 away from column faces. For a circular column, an equivalent square column of the same area can be used for b_o calculations. The equation was verified[3] with slab data having a broad range of relevant parameters. However, the applicability of the equation for slabs with very low reinforcement ratios and very thick slabs has not been verified thoroughly.

Muttoni[6] introduced the Critical Shear Crack Theory (CSCT) for calculating the punching shear strength of slabs without shear reinforcement. The method assumes that the punching shear strength V_{Rd} of a slab depends on the rotation ψ of the slab at failure, as well as crack width and aggregate interlock along the critical shear crack. The CSCT also considers that the rotation ψ of the slab depends on the applied punching shear force V and a few other parameters. Failure is reached when the applied punching shear force V is equal to the punching shear strength of the slab V_{Rd}.

The method requires an iterative solution to two equations: 1) the relationship between the punching shear strength V_{Rd} and rotation ψ; and 2) the relationship between the rotation ψ and applied shear force V. Equations (7) and (8) show these two equations

$$V_{Rd} = \frac{0.75}{1+15\dfrac{\psi d}{d_{go}+d_g}}\sqrt{f_c'}b_o d \quad \text{(SI units)}$$
$$V_{Rd} = \frac{9}{1+15\dfrac{\psi d}{d_{go}+d_g}}\sqrt{f_c'}b_o d \quad \text{(U.S. units)} \tag{7}$$

$$\psi = 1.5\frac{r_s}{d}\frac{f_y}{E_s}\left(\frac{V}{V_{flex}}\right)^{1.5} \tag{8}$$

where r_s is the radius of the slab (equal to half of a slab length or $0.22L$, where L is column-to-column span). V_{flex} is the shear force that will cause flexural failure of the slab. b_o is calculated at a distance $d/2$ away from column edges with round corners. d_{go} is set to be 16 mm and d_g is the maximum aggregate size. Muttoni[6] states that the size effect in CSCT is a function of r_s or slab span rather than the effective depth d.

The CSCT method can become complex, as it requires an iterative procedure to solve for V_{Rd}. In addition, every slab geometry, reinforcement ratio, and loading condition would lead to different yield line pattern, requiring yield line analysis to obtain V_{flex}. Consequently, for general design purposes, V_{flex} can be approximated[4,6] and taken equal to $8m$, where m is the moment capacity per unit width.

Peiris and Ghali[5] proposed a straightforward method to improve the ACI Code method by introducing a reduction factor, ρ/ρ_{fs}, to make it safer for slabs with low flexural reinforcement ratios. ρ_{fs} is the limiting reinforcement ratio. If the provided reinforcement ρ is reduced to below ρ_{fs}, the slab is assumed to fail in flexural mode instead of the usual punching mode. For slabs with provided reinforcement $\rho > \rho_{fs}$, the punching shear strength of the slab V_c is determined by the usual ACI equations (Eq. (1) to (3)). If the provided ρ in the slab is reduced below ρ_{fs}, the punching shear strength V_c becomes equal to V_{flex}—that is, the shear force that causes the slab to fail in flexural mode. For slabs with $\rho < \rho_{fs}$, Peiris and Ghali[5] assume that V_{flex} to be a linear function of ρ. So, the failure load for slabs with $\rho < \rho_{fs}$ is then equal to $(\rho/\rho_{fs})V_c$.

The key lies in the term ρ_{fs}. The V_{flex} can be calculated by using the yield line theory. For some simple cases, V_{flex} can be approximated[5] by $8m$, where m is moment capacity per unit width (ACI 318). By setting $V_{flex} = V_{c(ACI)}$, the ρ becomes ρ_{fs}, and the ρ_{fs} can be obtained. So

$$8m = 4\sqrt{f_c'}b_o d,\ \text{where}\ m = 0.95 f_y d^2\rho \tag{9}$$

Then, solving for ρ or ρ_{fs}

$$\rho_{fs} = \frac{4\sqrt{f_c'}b_o d}{8\times 0.95 f_y d^2}\ \text{(U.S. units)} \tag{10}$$

DERIVATION OF PROPOSED EQUATION

The authors' proposed equation shown in Eq. (15) is an extension of the punching shear strength formula that was previously introduced by Teng et al.,[3] shown earlier in Eq. (5). New reduction factors to consider low reinforcement ratio and size effect are added.

Factor for low reinforcement ratio, k_{RR}

The effect of low reinforcement ratio is treated in the same way as in Peiris and Ghali's approach. If the reinforcement ratio is less than ρ_{fs}, then the failure mode changes from punching to flexural mode and a reduction factor for low ρ is activated. A suitable yield line pattern is chosen based on the authors' experimental results to determine the flexural strength V_{flex} of slabs under punching load. Then, by setting the V_{flex} to be equal to V_c of Eq. (5) and taking into consideration the reduction factors for size effect and column rectangularity, the reduction factor k_{RR} for the effect of low reinforcement ratio can be written as (the complete derivation of the factor k_{RR} is given in the Appendix A,* which is included in the electronic version of the paper)

$$k_{RR} = (\rho/\rho_{fs})^{1/6} \tag{11}$$

where ρ is the provided reinforcement ratio; and ρ_{fs} is given by

$$\rho_{fs} = (0.01)\left[\frac{0.6k_{CR}k_{SZ}f_c'^{1/3}b_o d}{\alpha_o(0.95 f_y d^2)}(100)\right]^{3/2} \quad \text{(SI units)}$$
$$\rho_{fs} = (0.01)\left[\frac{16.6k_{CR}k_{SZ}f_c'^{1/3}b_o d}{\alpha_o(0.95 f_y d^2)}(100)\right]^{3/2} \quad \text{(U.S. units)} \tag{12a}$$

where k_{CR} and k_{SZ} are the reduction factors for column rectangularity ratio and size effect, respectively (they will be discussed in the following). $\alpha_o = [2(c_1 + c_2)/r + 2\pi]$ with r being the distance from the column face to the point load and it can be taken as 0.2 times span length.

*The Appendix is available at **www.concrete.org/publications** in PDF format, appended to the online version of the published paper. It is also available in hard copy from ACI headquarters for a fee equal to the cost of reproduction plus handling at the time of the request.

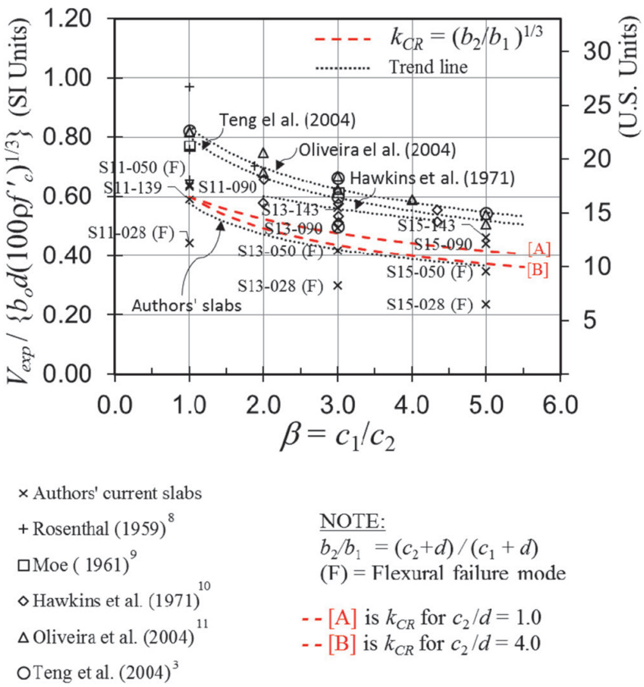

Fig. 7—Performance of proposed column rectangularity factor k_{CR}.

Note, however, that the general formula for ρ_{fs} given by Eq. (12a) can also be simplified considerably. By assuming typical values encountered in practice (refer to Appendix A), the simplified value of ρ_{fs} can be taken as

$$\rho_{fs} = 0.007 \text{ or } 0.7\% \tag{12b}$$

Thus, the authors now have two proposed methods: 1) the general method, which uses the ρ_{fs} of Eq. (12a); and 2) the simplified method, which uses ρ_{fs} of Eq. (12b). The simplified method will give equally accurate predictions of punching failure loads but less accurate predictions of failure modes.

Size effect and column rectangularity ratio

Various approaches have been employed to study the size effect in concrete structures. A fracture mechanics-based approach pioneered by Bažant et al.[7] leads to a reduction factor that is proportional to $d^{-1/2}$. However, due to the variability of test results, properties of concrete members, and the influence of reinforcement, an empirical approach is often used, and this can lead to a reduction factor that is proportional to $d^{-1/3}$ to $d^{-1/4}$ or others.

By observing the available experimental data and practical design considerations, the size-effect reduction factor k_{SZ} in the following is adopted for the proposed equation

$$k_{SZ} = (300/d)^{1/2} \leq 1.0 \quad \text{(SI units)}$$
$$k_{SZ} = (12/d)^{1/2} \leq 1.0 \quad \text{(U.S. units)} \tag{13}$$

k_{SZ} is chosen to be applicable for an effective depth $d >$ 300 mm (12 in.) simply because the current basic equation for V_c is safe for d of up to 300 mm (12 in.). For $d \leq 300$ mm (12 in.), $k_{SZ} = 1.0$. So, for the majority of slabs in practical structural design, the size effect factor can be disregarded.

For the column rectangularity ratio, β (= c_1/c_2), greater than 1.0, the corresponding reduction factor k_{CR} in Eq. (6), which was empirically derived, is retained with the exponent adjusted to 1/3 to suit more data

$$k_{CR} = (b_2/b_1)^{1/3} \tag{14}$$

Figure 7 shows the graph depicting the normalized shear stress at failure $V_{exp}/\{b_o d(100\rho f_c')^{1/3}\}$ against β (the ratio of long to short sides of the column, or c_1/c_2) for the authors' current slab specimens and other existing slab data from the literature.[3,8-11] Each of selected set of data comprises slab specimens with different column aspect ratios. The authors' slab specimens were made of high-strength concrete, while those from the literature were made of normal-strength concrete. It can be seen from the trend line for each set of data that the normalized shear stress decreases as the column aspect ratio increases. The trend lines are all similar to each other, including the one for the authors' current high-strength concrete slabs.

Figure 7 essentially shows the performance of the column rectangularity factor, k_{CR}, in comparison with experimental data. It can be seen that k_{CR} represents the trend line of the experimental data (including high-strength concrete slabs) very well. The way ACI treats rectangular column is by the use of the β coefficient as shown in Eq. (1). It cannot be shown together in Fig. 7 because ACI uses $\sqrt{f_c'}$ instead of $f_c'^{1/3}$ in its equation. Nevertheless, the ACI method of treating rectangular columns as shown in Eq. (1) also represents the experimental data very closely.

Proposed equation

The general form of the proposed equation can be written as

$$V_C = 0.6 k_{RR} k_{CR} k_{SZ} (100\rho f_c')^{1/3} b_o d \quad \text{(SI units)}$$
$$V_C = 16.6 k_{RR} k_{CR} k_{SZ} (100\rho f_c')^{1/3} b_o d \quad \text{(U.S. units)} \tag{15}$$

where k_{RR}, k_{CR}, and k_{SZ} are the reductions factors for reinforcement ratio, column rectangularity ratio, and size effect (refer to Eq. (11), (13), and (14)). ρ is A_s/bd and should not be taken greater than 2.5%. Note that in most cases, the reduction factors need not be calculated, as they will be equal to 1.

For commonly used slabs supported on square columns ($c_1/c_2 = 1$) with reinforcement ratios ρ greater than 0.7%, and effective depths d of 300 mm (12 in.) or less, the proposed equation in Eq. (15) becomes simple as follows

$$V_C = 0.6(100\rho f_c')^{1/3} b_o d \quad \text{(SI units)}$$
$$V_C = 16.6(100\rho f_c')^{1/3} b_o d \quad \text{(U.S. units)} \tag{16}$$

COMPARISON WITH EXPERIMENTAL RESULTS

Comparison with authors' 12 new high-strength concrete slab specimens

For the purpose of these comparisons, all the load factors, materials safety factors, and strength reduction factors are all set equal to 1.0. Shown in Table 2 are the punching shear strengths of the 12 high-strength concrete slabs presented earlier in this paper and the predictions of each of the methods discussed previously. It can be seen in Column (9) that the predictions of the ACI Code method are unconservative (V_{exp}/V_{calc} < 1.0) for slabs with low reinforcement ratios of 0.28% or 0.5%, as expected. For slabs with higher ρ, such as Sxy-090 and Sxy-143 series, the ACI predictions are conservative. The corrections to ACI method that was introduced by Peiris and Ghali[5] (Column (11)) make the corrected ACI method very conservative for low reinforcement ratio cases. For the Eurocode 2 predictions shown in Column (10), the predictions are reasonably conservative, but it cannot take into account the reduction in punching shear strengths of slabs supported on rectangular columns (S15 series especially) and of slabs with very low reinforcement ratio of < 0.3%, such as S11-028, S13-028, and S15-028. Muttoni et al.'s[6] CSCT method (Column 12) performs very well for these 12 slabs, with a coefficient of variation of only 8.4% and an average of V_{exp}/V_{calc} of 1.01.

The authors' proposed general prediction method (Column 13) is the most accurate, with an average of V_{exp}/V_c of 1.09 and a coefficient of variation of only 8.2%. The authors' proposed general prediction method can also predict the failure modes of the slabs accurately. Column (8) shows the values of ρ/ρ_{fs} from the standard ρ_{fs} equation (Eq. 12(a)). If the ρ/ρ_{fs} is less than 1.0, the corresponding slab would fail in flexural mode (F); otherwise, if ρ/ρ_{fs} is equal or greater than 1.0, the slab is expected to fail in punching (P). Column (6) shows the actual failure modes of the slabs. Comparing Column (8) and Column (6), it can be seen that the authors' general method predicts the actual failure modes very accurately—that is, all the failure modes are predicted correctly. In fact, both the general and the simplified methods predict the failure modes of the 12 HSC slabs correctly.

Comparison with slab database of 367 specimens

Table 3 summarizes the punching shear-strength predictions of the methods mentioned previously for the 367 slabs in the database. The material properties and complete details of the 367 slab data and the detailed comparisons of the failure load of each slab with the predictions of all the methods are given in Table A1 in Appendix B.

The current database of 367 slab data was from the authors' earlier database[3] with the addition of slab data from the database of the ACI Subcommittee 445-C[12] and new slab data from the literature shown in Table A1 in Appendix B. All the slab data in the current database is selected to make sure that they satisfy all the relevant ACI design requirements. Slabs having unusual geometries, loading arrangements, or boundary conditions were excluded, as their punching strengths would be quite different from those of normal slabs in typical construction and they deserve special treatment of their own.

The data are grouped according to three parameters (reinforcement ratio, effective depth, and compressive strength) and divided into three or four different divisions or ranges as detailed in Fig. 8 and 9 and also in Table 3. A good and reliable method is expected to perform well in all the different ranges or divisions.

Influence of reinforcement ratio—Figures 8(a) and (b) show the comparison between the experimental failure load V_{exp} and ACI 318-14[1] and Eurocode 2[2] predictions (V_{calc}), respectively. The ratio of the experimental failure load to the calculated punching shear strength (V_{exp}/V_{calc}) is plotted in the y-axis, with the x-axis being three design parameters: ρ, d, and f_c'. Separate statistical analysis is done for each of the divisions A1, A, B, and C. The horizontal dashed line in each division represents the average values of the V_{exp}/V_{calc} for that division. Figures 9(a), (b), and (c) show the comparisons of the experimental results with the predictions of CSCT,[6] Peiris-Ghali,[5] and the authors' general methods, respectively. The statistical analysis results for each division are summarized in a tabulated format in Table 3.

The performance of the ACI equations with respect to reinforcement ratio is shown in the leftmost chart in Fig. 8(a). It can be seen that as the reinforcement ratio increases, the average of V_{exp}/V_{calc} increases as well. Similarly, Table 3 shows for the ACI318-14 predictions that as the reinforcement ratio increases from Group A1 (Column (4) or ρ < 0.6%) to C (Column (7) or ρ > 2%), the average of the V_{exp}/V_{calc} increase from 0.86 to 1.61. This is caused by the neglect of the reinforcement ratio in the V_c formulas in the ACI 318-14. Note also that for the region A1(ρ <0.6%) in both Fig. 8(a) and Table 3, the average is 0.86 and most of the points are below the 1.0 line. This confirms the earlier conclusion from the 12 HSC slabs that the ACI 318 method for punching shear is unconservative for slabs with low reinforcement ratio, specifically for ρ less than approximately 0.6% or 0.7%.

The correction procedure introduced by Peiris-Ghali to take care of possible flexural failure prior to punching failure is effective for the intended A1 region. From Table 3, in Peiris-Ghali rows, the average of V_{exp}/V_{calc} in division A1 increases from 0.86 (ACI average) to a healthy 1.15. However, the maximum V_{exp}/V_{calc} increases from 1.19 to 2.42. This shows that the correction can also lead to overconservatism of the method. Both the Eurocode 2 (EC2) method and Muttoni et al.'s CSCT method give good predictions with the CSCT having slightly lower coefficients of variations (average COV, that is; average of the four divisions = 0.16 compared to 0.18 for EC2). Figure 9(a) shows that CSCT predictions in terms of reinforcement ratio has narrower band (better) compared to Fig. 8(b) for EC2. Note, however, that both methods have a minimum V_{exp}/V_{calc} of 0.64 for EC2 and 0.57 for the CSCT method. These are quite low.

The authors' proposed method can be considered the best with respect to reinforcement ratio. The combined average of V_{exp}/V_{calc} of the four divisions (sum of four averages divided by 4) is approximately 1.2, with a combined average COV of approximately 0.15. The leftmost chart of Fig. 9(c) shows the authors' predictions using the general method. The average of one division is close to the averages of the other three divisions, and the data are in a reasonably narrow band, indicating a low COV.

Influence of effective depth—The middle charts in Fig. 8 and 9 and Columns 8 to 10 of Table 3 show the statistical

Table 3—Comparison of experimental and calculated failure load by all methods

V_{exp}/V_{calc}			Reinforcement ratio ρ, %				Effective depth d, mm			Concrete strength f_c', MPa		
			[A1]	[A]	[B]	[C]	[A]	[B]	[C]	[A]	[B]	[C]
Division, units		All data	$\rho <$ 0.6%	$0 < \rho \leq$ 1.0%	$1.0 < \rho \leq$ 2.0%	$\rho >$ 2.0%	$d \leq 100$ mm	$100 < d <$ 300 mm	$d \geq 300$ mm	$f_c' \leq 50$ MPa	$50 < f_c' \leq$ 90 MPa	$f_c' > 90$ MPa
No. of data:		367	57	160	175	41	114	247	6	279	63	25
(1)	(2)	(3)	(4)	(5)	(6)	(7)	(8)	(9)	(10)	(11)	(12)	(13)
V_{exp}/V_{calc} ACI 318-14	Minimum	0.49	0.49	0.49	0.76	1.06	0.70	0.49	0.64	0.51	0.59	0.49
	Maximum	2.32	1.19	1.78	1.92	2.32	2.32	1.98	1.10	2.32	1.79	1.98
	Average	1.26	0.86	1.08	1.37	1.61	1.38	1.22	0.86	1.28	1.22	1.17
	Coefficient of variation	0.249	0.233	0.258	0.171	0.167	0.223	0.247	0.193	0.240	0.236	0.366
V_{exp}/V_{calc} Eurocode 2	Minimum	0.64	0.68	0.68	0.64	0.83	0.79	0.64	0.79	0.69	0.64	0.68
	Maximum	2.04	1.32	1.77	2.01	2.04	2.04	1.48	0.99	2.04	1.48	1.23
	Average	1.14	1.02	1.11	1.17	1.21	1.26	1.09	0.90	1.16	1.10	1.02
	Coefficient of variation	0.174	0.169	0.175	0.183	0.179	0.158	0.156	0.085	0.171	0.181	0.138
V_{exp}/V_{calc} CSCT	Minimum	0.57	0.64	0.64	0.57	0.76	0.65	0.57	0.68	0.64	0.57	0.89
	Maximum	1.82	1.37	1.37	2.19	1.38	1.82	1.48	1.21	1.82	1.31	1.23
	Average	1.04	1.02	1.03	1.06	1.02	1.07	1.02	0.86	1.04	1.02	1.04
	Coefficient of variation	0.152	0.17	0.145	0.198	0.129	0.156	0.145	0.22	0.151	0.174	0.094
V_{exp}/V_{calc} Peiris-Ghali	Minimum	0.75	0.76	0.75	0.76	1.06	0.90	0.76	0.75	0.75	0.76	0.94
	Maximum	2.42	2.42	2.42	2.31	2.32	2.32	2.42	1.10	2.32	1.79	2.42
	Average	1.31	1.15	1.19	1.37	1.61	1.42	1.28	0.89	1.32	1.23	1.47
	Coefficient of variation	0.214	0.27	0.217	0.177	0.167	0.185	0.215	0.152	0.201	0.217	0.282
V_{exp}/V_{calc} proposed Simplified Method	Minimum	0.73	0.73	0.73	0.76	0.83	0.86	0.73	1.16	0.73	0.83	0.97
	Maximum	1.69	1.55	1.67	1.69	1.50	1.69	1.67	1.28	1.69	1.56	1.43
	Average	1.21	1.18	1.22	1.22	1.16	1.28	1.18	1.23	1.21	1.24	1.16
	Coefficient of variation	0.151	0.151	0.151	0.151	0.153	0.127	0.158	0.031	0.150	0.160	0.131
V_{exp}/V_{calc} proposed General Method	Minimum	0.76	0.81	0.81	0.76	0.83	0.86	0.76	1.13	0.76	0.83	0.98
	Maximum	1.69	1.49	1.67	1.69	1.50	1.69	1.67	1.24	1.69	1.56	1.43
	Average	1.20	1.13	1.20	1.22	1.16	1.27	1.17	1.19	1.20	1.23	1.17
	Coefficient of variation	0.152	0.143	0.151	0.153	0.153	0.129	0.158	0.035	0.151	0.164	0.125

Notes: Regions A1, A, B, C correspond to the regions in Fig. 8 and 9. 1 mm = 0.0394 in., 1 MPa = 145.0 psi.

analysis results as they are influenced by the effective depth, d. It can be seen from the middle chart in Fig. 8(a) that the average of V_{exp}/V_{calc} of the ACI 318-14[1] becomes lower as the effective depth d increases. The ACI method can be unconservative for slabs having an effective depth of greater than 300 mm (12 in.). Obviously, this is caused by the neglect of size effect in the ACI equations. The Peiris-Ghali method, which is a correction to ACI method, does not address size effect.

The EC2[2] equation, which has a size effect term, also does not perform well when d is greater than 300 mm (12 in.) (refer to the middle chart in Fig. 8(b)). The CSCT method also does not predict well the punching shear strengths of slabs that are thicker than 300 mm (12 in.).

Both the authors' simplified and general methods show very good agreements with the experimental results. The average lines from the authors' general method across the different divisions of effective depths as shown in Fig. 9(c) are very close to each other, indicating a very good match between the equations and actual failure behavior of the slabs. The average of the three divisions is approximately 1.2 and the average COV is approximately 0.11 for both the simplified and standard equations.

Influence of compressive strength—The third charts (rightmost) in Fig. 8(a) shows the performance of ACI method in terms of compressive strength f_c'. It can be seen that the average of V_{exp}/V_{calc} in one division or range (represented by the horizontal dashed line) is nearly the same as that of

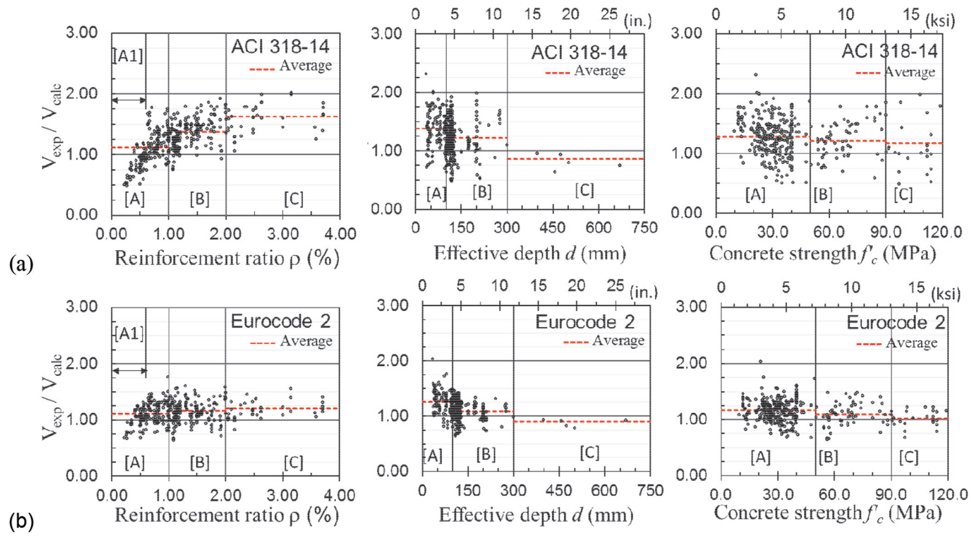

Fig. 8—Failure load predictions of 367 test data by: (a) ACI 318-14; and (b) Eurocode 2 2004.

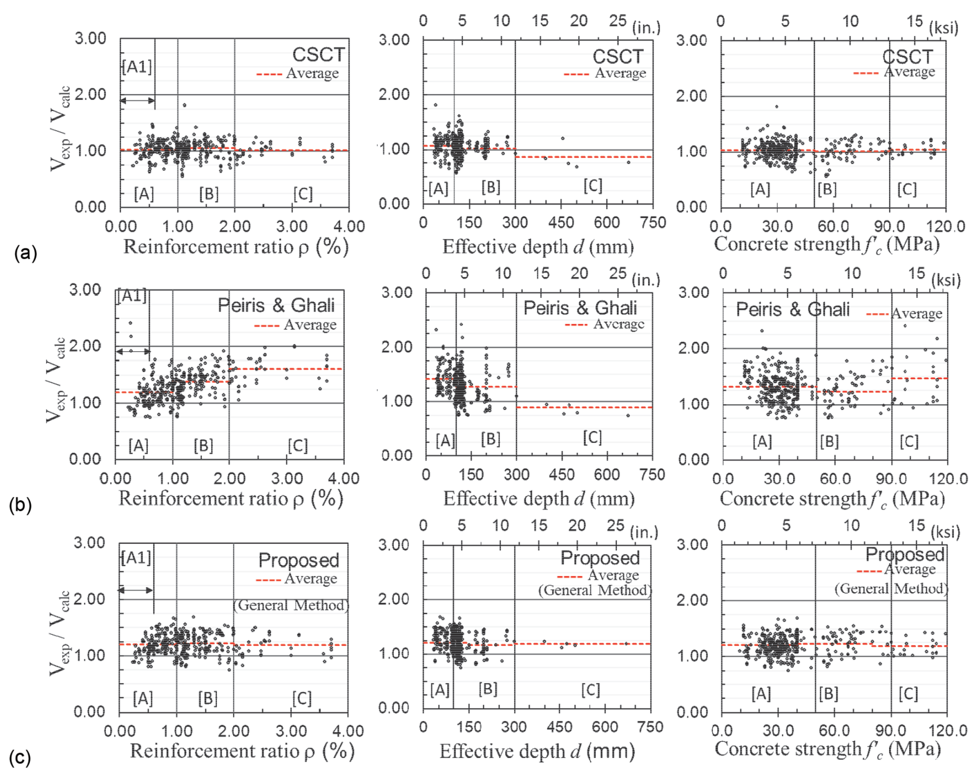

Fig. 9—Failure load predictions of 367 test data by: (a) CSCT; (b) Peiris and Ghali; and (c) Authors' proposed General Method.

the other divisions. This is true for the other four methods shown in Fig. 8(b) and 9(a), (b), and (c). However, the ACI method has the widest spread of results with combined COV across the three divisions of 0.28. The CSCT method provides the best predictions with a combined average of V_{exp}/V_{calc} of 1.03 and with a combined COV of 0.14. The authors' simplified and general prediction equations both have a combined average of 1.2 and a combined COV of 0.15. Both CSCT and the authors' methods can be considered equally accurate. Table 3 (Column 13, for $f_c' > 90$ MPa [13,000 psi]) shows that the CSCT method predicts the punching shear strength of HSC slabs ($f_c' > 90$ MPa [13,000 psi]) very well with an average of 1.04 and a COV of 0.094. The next best method for $f_c' > 90$ MPa [13,000 psi] is the authors' general and simplified methods with the COVs of 0.125 and 0.131, respectively, followed by the EC2, Peiris-Ghali, and ACI methods.

Other parameters, failure modes, and summary—It is understood that influencing parameters can be interrelated and they may also influence each other. These are considered as much as possible. Other parameters that might influence the punching shear strength include column size to slab thickness effect (c/d or b_o/d), maximum aggregate size d_a, and also shear span-depth ratio (r/d or $0.2L/d$). However, those effects were insignificant.

From the aforementioned comparative study, it can be seen that the authors' proposed General Method and the Simplified Method are accurate and reliable. The General

Method predicts failure modes more accurately than the Simplified Method (refer to Table A1 in Appendix B). Of the 27 slabs that failed in flexure, the general method correctly predicted 20 of them (74% correct) while the simplified method predicts 21 correctly (78%). Of the 340 slabs failing in punching, the general method predicts mode of failure correctly for 316 (93%) of them compared to 274 (81%) for the simplified method. Nevertheless, both methods predict the punching shear strength equally accurately and they give the closest predictions to the experimental failure loads compared to other methods. The simplified method is especially very simple to use.

CONCLUSIONS

Based on the authors' experiments and the accompanying discussion as well as the comparative study of six different methods against the database of 367 slabs, the following conclusions can be made; they are applicable to normal-strength as well as high-strength concrete slabs:

1. Under a punching load, a slab provided with a low reinforcement ratio (approximately less than 0.6 to 0.7%) may fail in flexure first before it fails in what looks like punching failure in the end. The failure mode will be ductile and the failure load will be the load that causes yielding of the majority of the reinforcement. The failure load will be lower than predicted by ACI 318-14 equations for punching shear.

2. Slabs failing in pure punching shear mode will tend to form circular-fan-type crack patterns at failure, while those failing in flexural mode will tend to form cracks parallel to column lines. In this case, the final circumferential crack tends to be very close to the column.

3. The higher the amount of reinforcement provided, the higher the failure load. However, only those reinforcements within the width of $1.5h$ from a column face (or total width of $c_2 + 3h$ for an interior column) will be fully effective in resisting punching shear stresses and, therefore, can be considered in influencing the punching shear strength.

4. The ACI 318 method is unconservative for slabs with low reinforcement ratios (especially for $\rho < 0.7\%$). The correction procedure proposed by Peiris and Ghali fixes the problem but it may lead to over-conservatism. The EC2 method can be unconservative for slabs with very low reinforcement ratio and supported on rectangular columns.

5. The ACI 318, EC2, and CSCT methods may not be safe for slabs with an effective depth of more than 300 mm (12 in.), even though EC2 and CSCT do consider size effect. ACI needs to consider the inclusion of size effect into the equation.

6. The authors' general method and simplified method both have been shown to be most accurate and reliable with uniform averages of V_{exp}/V_{calc} and COV across different ranges of design parameters. The simplified method is especially simple to use.

AUTHOR BIOS

ACI member **Susanto Teng** *is an Associate Professor at the School of Civil and Environmental Engineering, Nanyang Technological University (NTU), Singapore. He is a member of ACI Committee 435, Deflection of Concrete Building Structures, and Joint ACI-ASCE Committees 421, Design of Reinforced Concrete Slabs, and 445, Shear and Torsion. His research interests include shear in beams, slab-column connections, finite element modeling, and tall buildings.*

Khatthanam Chanthabouala *is a PhD Candidate in the School of Civil and Environmental Engineering at NTU. His research interests include punching shear strength of high-strength concrete and steel fiber-reinforced concrete slabs.*

Darren T. Y. Lim *is a PhD Candidate in the School of Civil and Environmental Engineering at NTU. His research interests include concrete technology and shear behavior of large concrete beams.*

Rhahmadatul Hidayat *is a Civil Engineer with Mott MacDonald Consultants, Singapore. He received his master's degree from NTU. His research interests include tunnel construction for the underground Mass Rapid Transit system in Singapore.*

ACKNOWLEDGMENTS

This research was made possible by the funding provided by the National Research Foundation (NRF) of Singapore and the support of Nanyang Technological University, Singapore.

REFERENCES

1. ACI Committee 318, "Building Code Requirements for Structural Concrete (ACI 318-14) and Commentary (ACI 318R-14)," American Concrete Institute, Farmington Hills, MI, 2014, 519 pp.

2. CEN, "Eurocode 2—Design of Concrete Structures: Part 1-1—General Rules and Rules for Buildings," EN 1992-1-1, Brussels, Belgium, 2004, 225 pp.

3. Teng, S.; Cheong, H. K.; Kuang, K. L.; and Geng, J. Z., "Punching Shear Strength of Slabs with Openings and Supported on Rectangular Columns," *ACI Structural Journal*, V. 101, No. 5, Sept.-Oct. 2004, pp. 678-687.

4. Guandalini, S.; Burdet, O. L.; and Muttoni, A., "Punching of Slabs with Low Reinforcement Ratios," *ACI Structural Journal*, V. 106, No. 1, Jan.-Feb. 2009, pp. 87-95.

5. Peiris, C., and Ghali, A., "Flexural Reinforcement Essential for Punching Shear Resistance of Slabs," *Recent Development in Reinforced Concrete Slab Analysis, Design, and Serviceability*, SP-287, M. Mahamid and F. Malhas, eds., American Concrete Institute, Farmington Hills, MI, 2012, pp. 1-16.

6. Muttoni, A., "Punching Shear Strength of Reinforced Concrete Slabs without Transverse Reinforcement," *ACI Structural Journal*, V. 105, No. 4, July-Aug. 2008, pp. 440-450.

7. Bažant, Z. P.; Yu, Q.; Gerstle, W.; Hanson, J.; and Ju, J. W., "Justification of ACI 446 Proposal for Updating ACI Code Provisions for Shear Design of Reinforced Concrete Beams," *ACI Structural Journal*, V. 104, No. 5, Sept.-Oct. 2007, pp. 601-610.

8. Rosenthal, I., "Experimental Investigation of Flat Plate Floors," *ACI Journal Proceedings*, V. 56, No. 12, Dec. 1959, pp. 153-166.

9. Moe, J., "Shearing Strength of Reinforced Concrete Slabs and Footings under Concentrated Loads," *Bulletin D47*, Portland Cement Association, Research and Development Laboratories, Skokie, IL, 1961, 130 pp.

10. Hawkins, N. M.; Fallsen, H. B.; and Hinojosa, R. C., "Influence of Column Rectangularity on the Behaviour of Flat Plate Structures," *Cracking, Deflection, and Ultimate Load of Concrete Slab Systems*, SP-30, American Concrete Institute, Farmington Hills, MI, 1971, pp. 677-720.

11. Oliveira, D. R. C.; Regan, P. E.; and Melo, G. S. S. A., "Punching Resistance of RC Slabs with Rectangular Columns," *Magazine of Concrete Research*, V. 56, No. 3, 2004, pp. 123-138. doi: 10.1680/macr.2004.56.3.123

12. Ospina, C. E.; Birkle, G.; Widianto; and Kuchma, D., "ACI 445C - Punching Shear - Collected Databank," 2011, https://nees.org/resources/3660/. (last accessed Dec. 18, 2017)

APPENDIX A

A Derivation of the factor for low reinforcement ratio, k_{RR}

The idealized yield line pattern that can represent the transition phase from punching mode to flexural mode is shown in **Fig. A1**. The V_{flex} for the slab with that yield line pattern can be obtained (see Park and Gamble[13]) and is given by:

$$V_{flex} = \alpha_o m, \quad \text{where } \alpha_o = [2(c_1 + c_2)/r + 2\pi] \text{ and } m = 0.95\, \rho_{fs} f_y\, d^2 \qquad \text{(A1)}$$

c_1 and c_2 are the lengths of long and short sides of column cross-section, respectively. r is the distance from the column face to the point load (for design purpose, r can be assumed to be $0.2L$, that is the distance from the column to the inflection point in a flat plate floor).

The limiting reinforcement ratio ρ_{fs} can be obtained by setting $V_{flex} = V_c$, that is, Eq. (A1) = Eq. (5) in the main text. Adding the reduction factor k_{SZ} for size effect to Eq. (5), the following is obtained (note that ρ has become ρ_{fs}):

$$\alpha_o (0.95\, \rho_{fs} f_y\, d^2) = 0.6\, k_{CR}\, k_{SZ}\, (100\rho_{fs} f'_c)^{1/3} b_o d$$

The ρ_{fs} ($= A_s/bd$) is then obtained as

$$100\rho_{fs} = \left[\frac{0.6 k_{CR} k_{SZ} f_c'^{1/3} b_o d}{\alpha_o (0.95 f_y d^2)}(100)\right]^{3/2} \text{(SI Units)}; \; = \left[\frac{16.6 k_{CR} k_{SZ} f_c'^{1/3} b_o d}{\alpha_o (0.95 f_y d^2)}(100)\right]^{3/2} \text{(US Units)}$$

(A2a)

The yield line pattern shown in **Fig. A1** is to represent slabs supported on square as well as rectangular columns. The actual value of α_o varies from about 8 for square columns to about 10 for rectangular columns.

Note, however, that the standard ρ_{fs} of Eq. (A2a) can be simplified considerably, if desired. By assuming α_o to be equal to 8, the two reduction factors to be 1.0, f'_c = 40 MPa (5800 psi), f_y = 410

MPa (60 ksi), column size c_1 and c_2 = 350 mm (13.8 in.), d = 175 mm (6.9 in), the value of ρ_{fs} becomes 0.007 or

$$100\rho_{fs} = \left[\frac{0.6(1)(1)(40)^{1/3}(2100)(175)}{(8)(0.95)(410)(175)^2)}(100)\right]^{3/2} \approx 0.7 \qquad \text{(A2b)}$$

For slabs with low reinforcement ratios or ρ less than ρ_{fs}, **Fig. A2** is constructed. In **Fig.A2**, the x-axis is the reinforcement ratio ρ and the y-axis is $V_{exp}/\{0.6\, k_{CR}\, k_{SZ}\, (f'_c)^{1/3}\, b_o d\}$ (SI units) or $V_{exp}/\{16.6\, k_{CR}\, k_{SZ}\, (f'_c)^{1/3}\, b_o d\}$ (U.S. units). Experimental slab data that failed in flexure are plotted in **Fig. A2.** The denominator is essentially V_c of Eq. (1) without the $\rho^{1/3}$ term. A solid line is also drawn from the origin to an arbitrary point of ρ = 0.7%. Since, in **Fig. A2**, at ρ = 0.7% the y-axis is equal to 1.0, this ρ is actually ρ_{fs} where $V_{flex} = V_c$. So, taking ρ_{fs} = 0.7% and assuming that the punching shear strength to be a linear function of ρ, for $\rho < \rho_{fs}$, produces the solid inclined line. A more suitable form for the relationship between failure load and ρ for the region of $\rho < \rho_{fs}$ would be a function of $(\rho/\rho_{fs})^{1/2}$ as shown by the curved line (**Fig. A2**). Therefore, a reduction factor for low reinforcement ratio is needed for the region of $\rho < \rho_{fs}$. The punching shear strength of the slab would best be represented by $k_{RR}V_c$, where $k_{RR} = (\rho/\rho_{fs})^{1/2}$. Since the basic form of V_c itself (Eq. (5)) has already had $\rho^{1/3}$ term in it, the exponent in k_{RR} needs to be reduced by 1/3, which is the exponent of ρ in basic V_c, to become (1/2 - 1/3) = 1/6, or

$$k_{RR} = (\rho/\rho_{fs})^{1/6} \qquad \text{(A3)}$$

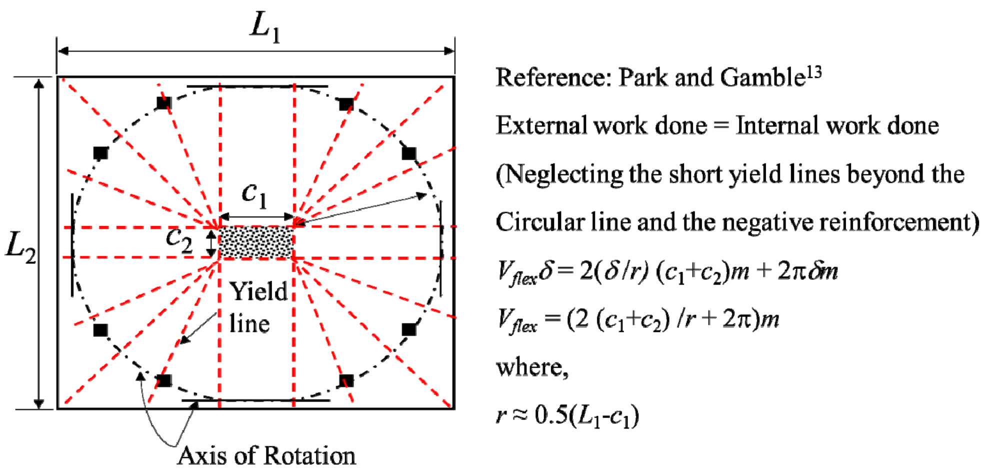

Fig. A1 *– Idealized yield line pattern representing transition from punching failure mode to flexural failure mode.*

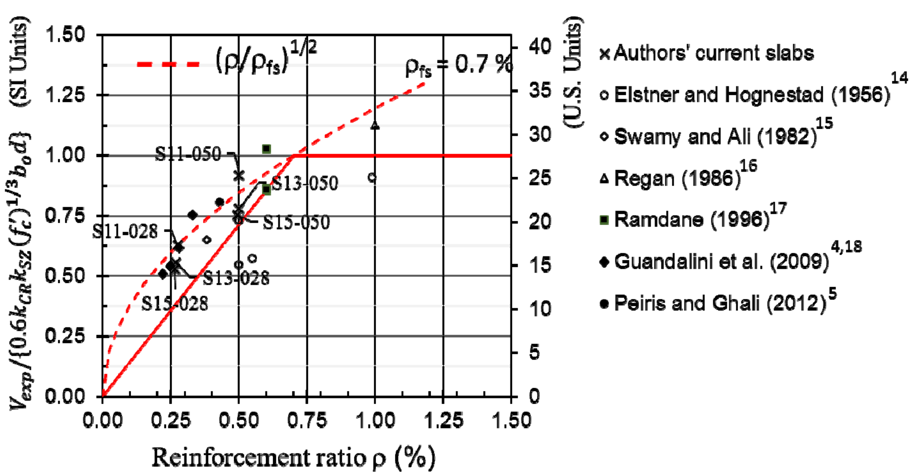

Fig. A2 *– Relationship between V_{exp} and ρ for slabs with low reinforcement ratios* ρ.

APPENDIX B

Table A1 (Columns (2) to (15)) shows the original slab ID, material properties, observed failure mode and failure load V_{exp} of 367 slab data including the current 12 high strength concrete slabs. Columns (16) and (17) of **Table A1** show the failure mode predictions by the proposed simplified and general methods, respectively. Columns (18) to (23) show the ratio of the failure load to the calculated punching shear strength V_{exp}/V_{calc} of each design method such as ACI 318-14[1], Eurocode 2[2], Critical Shear Crack Theory by Muttoni[6], Peiris and Ghali[5], and the proposed simplified and general methods, respectively.

All the slab data in **Table A1** was constructed without shear reinforcement and tested under punching shear loads to failures. They were selected to make sure that they satisfy all the relevant ACI design requirements. Slabs having unusual geometries, loading arrangements, or boundary conditions were excluded as their punching strengths would be quite different from those of normal slabs in typical construction and they deserve special treatment of their own. The ranges of the parameters of the 367 slab data can be summarized as follows:

- The slab lengths L_1 and L_2 range from 483 to 6000 mm (1.60 to 19.70 ft).
- The column dimensions (c_1, c_2) range from 50 to 1000 mm (2.0 to 39.4 in.), which include column shapes such as square (denoted as "S"), rectangular ("R") and circular s ("C").
- The average effective depth d ranges from 33 to 669 mm (1.3 to 26.4 in.).
- The average reinforcement ratio ρ ranges from 0.22 to 7.30%.
- The (cylinder) concrete strength f'_c ranges from 9.5 to 119 MPa (1378 to 17260 psi).
- The yield strength of the reinforcement f_y ranges from 255 to 749 MPa (37 to 110 ksi).

Table A1 -- Properties of 367 slab data and Comparison of design methods

No.	Year	Ref. [No.]	Slab ID	L_1 (mm)	L_2 (mm)	c_1 (mm)	c_2 (mm)	Column Shape	d (mm)	f'_c (MPa)	f_y (MPa)	ρ (%)	V_{exp} (kN)	Failure mode	ρ/ρ_{fs} Simplified Method	ρ/ρ_{fs} General Method	V_{exp}/V_{calc} ACI 318-14	V_{exp}/V_{calc} Eurocode 2	V_{exp}/V_{calc} CSCT	V_{exp}/V_{calc} Peiris-Ghali	V_{exp}/V_{calc} Proposed Simple Method	V_{exp}/V_{calc} Proposed General Method
(1)	(2)	(3)	(4)	(5)	(6)	(7)	(8)	(9)	(10)	(11)	(12)	(13)	(14)	(15)	(16)	(17)	(18)	(19)	(20)	(21)	(22)	(23)
1	1938	[19]	1362	1700	1700	300	300	S	271	12.3	270	1.04	1165	P	1.49	2.55	1.61	1.19	1.13	1.61	1.34	1.34
2	1938	[19]	1375	1700	1700	300	300	S	473	13.1	270	0.60	1659	P	0.86	2.94	0.94	0.83	0.74	0.94	1.23	1.20
3	1946	[20]	1	1200	1200	140	140	C	101	11.5	350	0.70	183.0	P	1.00	1.83	1.78	1.47	1.22	1.78	1.56	1.56
4	1946	[20]	2	1200	1200	140	140	C	111	11.5	350	0.64	177.0	P	0.91	1.81	1.50	1.24	1.05	1.50	1.38	1.36
5	1946	[20]	3	1200	1200	140	140	C	106	11.5	350	0.67	172.0	P	0.95	1.82	1.56	1.29	1.08	1.56	1.40	1.39
6	1946	[20]	4	1200	1200	140	140	C	110	11.5	350	0.64	177.0	P	0.92	1.81	1.52	1.26	1.06	1.52	1.40	1.38
7	1946	[20]	5	1200	1200	140	140	C	111	11.5	350	0.64	198.0	P	0.91	1.81	1.68	1.39	1.17	1.68	1.55	1.52
8	1946	[20]	6	1200	1200	140	140	C	107	11.5	350	0.66	183.0	P	0.94	1.82	1.63	1.35	1.13	1.63	1.48	1.47
9	1946	[20]	7	1200	1200	140	140	C	106	11.5	350	0.67	187.0	P	0.95	1.82	1.69	1.40	1.17	1.69	1.53	1.51
10	1956	[14]	A-1a	1829	1829	254	254	S	118	14.1	332	1.15	302.5	P	1.64	1.73	1.38	1.13	1.04	1.38	1.14	1.14
11	1956	[14]	A-1b	1829	1829	254	254	S	118	25.2	332	1.15	364.7	P	1.64	1.29	1.25	1.13	1.02	1.25	1.13	1.13
12	1956	[14]	A-1c	1829	1829	254	254	S	118	29.0	332	1.15	355.8	P	1.64	1.20	1.13	1.05	0.95	1.13	1.05	1.05
13	1956	[14]	A-1d	1829	1829	254	254	S	118	36.8	332	1.15	351.4	P	1.64	1.07	0.99	0.96	0.87	0.99	0.96	0.96
14	1956	[14]	A-1e	1829	1829	254	254	S	118	20.3	332	1.15	355.8	P	1.64	1.44	1.36	1.18	1.08	1.36	1.19	1.19
15	1956	[14]	A-2a	1829	1829	254	254	S	114	13.7	321	2.47	333.6	P	3.53	3.48	1.61	1.10	1.02	1.61	1.02	1.02
16	1956	[14]	A-2b	1829	1829	254	254	S	114	19.5	321	2.47	400.3	P	3.53	2.91	1.62	1.17	1.04	1.62	1.09	1.09
17	1956	[14]	A-2c	1829	1829	254	254	S	114	37.4	321	2.47	467.0	P	3.53	2.10	1.36	1.10	0.93	1.36	1.02	1.02

No.	Year	Ref. [No.]	Slab ID	L_1 (mm)	L_2 (mm)	c_1 (mm)	c_2 (mm)	Column Shape	d (mm)	f'_c (MPa)	f_y (MPa)	ρ (%)	V_{exp} (kN)	Failure mode	ρ/ρ_{fs} Simplified Method	ρ/ρ_{fs} General Method	V_{exp}/V_{calc} ACI 318-14	Eurocode 2	CSCT	Peiris-Ghali	Proposed Simple Method	Proposed General Method
(1)	(2)	(3)	(4)	(5)	(6)	(7)	(8)	(9)	(10)	(11)	(12)	(13)	(14)	(15)	(16)	(17)	(18)	(19)	(20)	(21)	(22)	(23)
18	1956	[14]	A-7b	1829	1829	254	254	S	114	27.9	321	2.47	511.5	P	3.53	2.44	1.73	1.33	1.15	1.73	1.23	1.23
19	1956	[14]	A-3a	1829	1829	254	254	S	114	12.8	321	3.70	355.8	P	5.29	5.39	1.77	1.20	1.08	1.77	1.11	1.11
20	1956	[14]	A-3b	1829	1829	254	254	S	114	22.6	321	3.70	444.8	P	5.29	4.05	1.67	1.24	1.01	1.67	1.15	1.15
21	1956	[14]	A-3c	1829	1829	254	254	S	114	26.5	321	3.70	533.8	P	5.29	3.74	1.85	1.41	1.12	1.85	1.31	1.31
22	1956	[14]	A-3d	1829	1829	254	254	S	114	34.5	321	3.70	547.1	P	5.29	3.28	1.66	1.32	1.03	1.66	1.23	1.23
23	1956	[14]	A-4	1829	1829	356	356	S	118	26.1	332	1.15	400.3	P	1.64	1.00	1.06	1.05	0.95	1.06	0.96	0.96
24	1956	[14]	A-5	1829	1829	356	356	S	114	27.8	321	2.47	533.8	P	3.53	1.92	1.41	1.19	1.00	1.41	1.01	1.01
25	1956	[14]	A-6	1829	1829	356	356	S	114	25.0	321	3.70	498.2	P	5.29	3.03	1.39	1.15	0.89	1.39	0.97	0.97
26	1956	[14]	A-9	1829	1829	254	254	S	114	29.9	321	3.56	444.8	P	5.09	3.39	1.45	1.13	0.89	1.45	1.05	1.05
27	1956	[14]	A-10	1829	1829	356	356	S	114	29.7	321	3.58	489.3	P	5.11	2.69	1.25	1.07	0.82	1.25	0.90	0.90
28	1956	[14]	A-13	1829	1829	356	356	S	121	26.2	294	0.55	235.7	F	0.79	0.41	0.60	0.76	0.75	1.30	0.73	0.81
29	1956	[14]	B-1	1829	1829	254	254	S	114	14.2	324	0.50	178.4	F	0.71	0.70	0.84	0.92	0.81	1.13	0.97	0.98
30	1956	[14]	B-2	1829	1829	254	254	S	114	47.6	321	0.50	200.2	F	0.71	0.38	0.52	0.69	0.64	1.22	0.73	0.81
31	1956	[14]	B-4	1829	1829	254	254	S	114	47.7	303	0.99	333.6	F	1.41	0.68	0.86	0.92	0.79	1.10	0.91	0.97
32	1956	[14]	B-9	1829	1829	254	254	S	114	43.9	341	2.00	504.8	P	2.86	1.72	1.36	1.13	0.95	1.36	1.12	1.12
33	1956	[14]	B-11	1829	1829	254	254	S	114	13.5	409	3.00	329.2	P	4.29	6.11	1.60	1.09	0.96	1.60	1.01	1.01
34	1956	[14]	B-14	1829	1829	254	254	S	114	50.5	325	3.00	578.2	P	4.29	2.24	1.45	1.23	0.93	1.45	1.14	1.14
35	1959	[8]	II/1	1143	1143	229	229	C	80	13.7	456	1.34	181.0	P	1.91	2.94	1.62	1.38	1.15	1.62	1.16	1.16
36	1959	[8]	II/2	1702	1702	229	229	C	80	12.7	372	1.32	152.0	P	1.89	1.87	1.41	1.20	1.11	1.41	1.00	1.00

No.	Year	Ref. [No.]	Slab ID	L_1 (mm)	L_2 (mm)	c_1 (mm)	c_2 (mm)	Column Shape	d (mm)	f'_c (MPa)	f_y (MPa)	ρ (%)	V_{exp} (kN)	Failure mode	ρ/ρ_{fs} Simplified Method	ρ/ρ_{fs} General Method	V_{exp}/V_{calc}					
																	ACI 318-14	Eurocode 2	CSCT	Peiris-Ghali	Proposed Simple Method	Proposed General Method
(1)	(2)	(3)	(4)	(5)	(6)	(7)	(8)	(9)	(10)	(11)	(12)	(13)	(14)	(15)	(16)	(17)	(18)	(19)	(20)	(21)	(22)	(23)
37	1959	[8]	II/3	1702	1702	432	229	R	80	14.2	490	1.32	245.0	P	1.89	2.53	1.50	1.38	1.43	1.50	1.38	1.38
38	1959	[8]	II/4	1143	1143	229	229	C	80	22.3	490	0.98	245.0	P	1.40	1.88	1.72	1.77	1.42	1.72	1.48	1.48
39	1960	[21]	IA15a-5	1840	1840	150	150	C	117	27.9	441	0.80	255.0	P	1.14	1.90	1.24	1.11	0.93	1.24	1.21	1.21
40	1960	[21]	IA15a-6	1840	1840	150	150	C	118	25.8	454	0.80	275.0	P	1.14	2.07	1.37	1.21	1.01	1.37	1.32	1.32
41	1960	[21]	IA15c-11	1840	1840	150	150	C	121	31.4	436	1.80	334.0	P	2.57	4.06	1.45	1.00	0.88	1.45	1.11	1.11
42	1960	[21]	IA15c-12	1840	1840	150	150	C	122	28.8	439	1.70	332.0	P	2.43	4.08	1.49	1.03	0.90	1.49	1.14	1.14
43	1960	[21]	IA30a-24	1840	1840	300	300	C	128	25.9	456	1.00	430.0	P	1.43	1.76	1.26	1.24	0.96	1.26	1.11	1.11
44	1960	[21]	IA30a-25	1840	1840	300	300	C	124	24.6	451	1.10	408.0	P	1.57	1.89	1.28	1.22	0.94	1.28	1.08	1.08
45	1960	[21]	IA30c-30	1840	1840	300	300	C	120	29.5	436	2.10	491.0	P	3.00	3.02	1.46	1.19	0.92	1.46	1.03	1.03
46	1960	[21]	IA30c-31	1840	1840	300	300	C	119	29.5	448	2.10	540.0	P	3.00	3.12	1.63	1.33	1.02	1.63	1.14	1.14
47	1960	[21]	IA30d-32	1840	1840	300	300	C	123	25.8	448	0.50	258.0	P	0.71	0.82	0.80	1.00	0.81	1.00	0.93	0.91
48	1960	[21]	IA30d-33	1840	1840	300	300	C	125	26.2	462	0.50	258.0	P	0.71	0.87	0.77	0.97	0.78	0.94	0.91	0.88
49	1960	[21]	IA30e-34	1840	1840	300	300	C	120	26.9	461	1.00	332.0	P	1.43	1.64	1.04	1.05	0.80	1.04	0.92	0.92
50	1960	[21]	IA30e-35	1840	1840	300	300	C	122	24.6	459	1.00	332.0	P	1.43	1.73	1.06	1.05	0.81	1.06	0.92	0.92
51	1961	[9]	H1	1830	1830	254	254	S	114	26.1	328	1.15	375.0	P	1.64	1.21	1.31	1.20	1.02	1.31	1.19	1.19
52	1961	[9]	S1-60	1830	1830	254	254	S	114	23.3	399	1.06	389.2	P	1.51	1.58	1.44	1.33	1.11	1.44	1.32	1.32
53	1961	[9]	S2-60	1830	1830	254	254	S	114	22.1	399	1.03	355.8	P	1.47	1.58	1.35	1.24	1.04	1.35	1.24	1.24
54	1961	[9]	S3-60	1830	1830	254	254	S	114	22.6	399	1.02	363.6	P	1.46	1.55	1.36	1.27	1.06	1.36	1.26	1.26
55	1961	[9]	S4-60	1830	1830	254	254	S	114	23.9	399	1.13	333.6	P	1.61	1.67	1.22	1.10	0.92	1.22	1.10	1.10

No.	Year	Ref. [No.]	Slab ID	L_1 (mm)	L_2 (mm)	c_1 (mm)	c_2 (mm)	Column Shape	d (mm)	f'_c (MPa)	f_y (MPa)	ρ (%)	V_{exp} (kN)	Failure mode	ρ/ρ_{fs} Simplified Method	ρ/ρ_{fs} General Method	V_{exp}/V_{calc} ACI 318-14	Eurocode 2	CSCT	Peiris-Ghali	Proposed Simple Method	Proposed General Method
(1)	(2)	(3)	(4)	(5)	(6)	(7)	(8)	(9)	(10)	(11)	(12)	(13)	(14)	(15)	(16)	(17)	(18)	(19)	(20)	(21)	(22)	(23)
56	1961	[9]	S1-70	1830	1830	254	254	S	114	24.5	482	1.06	392.3	P	1.51	2.05	1.41	1.31	1.08	1.41	1.31	1.31
57	1961	[9]	S3-70	1830	1830	254	254	S	114	25.4	482	1.02	378.1	P	1.46	1.94	1.34	1.27	1.04	1.34	1.26	1.26
58	1961	[9]	S4-70	1830	1830	254	254	S	114	35.2	482	1.13	373.6	P	1.61	1.82	1.12	1.08	0.89	1.12	1.08	1.08
59	1961	[9]	S4A-70	1830	1830	254	254	S	114	20.5	482	1.13	311.4	P	1.61	2.39	1.23	1.08	0.90	1.23	1.08	1.08
60	1961	[9]	S5-60	1830	1830	203	203	S	114	22.2	399	1.06	342.5	P	1.52	1.91	1.50	1.29	1.10	1.50	1.37	1.37
61	1961	[9]	S5-70	1830	1830	203	203	S	114	24.3	482	1.06	378.1	P	1.52	2.42	1.59	1.38	1.16	1.59	1.47	1.47
62	1961	[9]	R-1	1830	1830	457	152	R	114	27.6	328	1.38	393.6	P	1.97	1.87	1.41	1.08	1.11	1.41	1.32	1.32
63	1961	[9]	R-2	1830	1830	152	152	S	114	26.5	328	1.38	311.4	P	1.97	2.07	1.49	1.11	1.19	1.49	1.28	1.28
64	1961	[9]	M1A	1830	1830	305	305	S	114	23.0	481	1.50	432.8	P	2.14	2.62	1.41	1.22	1.01	1.41	1.16	1.16
65	1965	[22]	2S2	889	889	51	51	S	57	25.9	376	1.57	71.7	P	2.24	3.81	1.71	1.10	1.07	1.71	1.41	1.41
66	1965	[22]	2S3	889	889	76	76	S	57	24.5	376	1.57	91.1	P	2.25	3.03	1.81	1.28	1.17	1.81	1.47	1.47
67	1965	[22]	2S4	889	889	102	102	S	57	23.2	376	1.57	85.8	P	2.25	2.55	1.47	1.12	0.98	1.47	1.19	1.19
68	1965	[22]	2S5	889	889	127	127	S	57	22.1	376	1.57	96.5	P	2.24	2.22	1.46	1.17	1.01	1.46	1.17	1.17
69	1965	[22]	2S6	889	889	152	152	S	57	18.4	376	1.57	96.5	P	2.24	2.14	1.41	1.15	0.99	1.41	1.09	1.09
70	1965	[22]	3S2	889	889	51	51	S	57	22.8	376	3.14	78.4	P	4.49	8.12	1.99	1.16	1.12	1.99	1.37	1.37
71	1965	[22]	3S4	889	889	102	102	S	57	22.6	376	3.14	115.2	P	4.49	5.16	2.00	1.40	1.17	2.00	1.38	1.38
72	1965	[22]	3S6	889	889	152	152	S	57	21.6	376	3.14	149.9	P	4.49	3.95	2.02	1.56	1.23	2.02	1.38	1.38
73	1966	[23]	A1/M1	1370	1370	203	203	S	114	15.5	255	1.10	316.0	F	1.57	1.30	1.67	1.33	1.22	1.67	1.42	1.42
74	1966	[23]	A1/M2	1370	1370	203	203	S	117	14.7	282	1.50	339.0	P	2.14	2.17	1.77	1.26	1.17	1.77	1.34	1.34

No.	Year	Ref. [No.]	Slab ID	L_1 (mm)	L_2 (mm)	c_1 (mm)	c_2 (mm)	Column Shape	d (mm)	f'_c (MPa)	f_y (MPa)	ρ (%)	V_{exp} (kN)	Failure mode	ρ/ρ_{fs} Simplified Method	ρ/ρ_{fs} General Method	V_{exp}/V_{calc} ACI 318-14	Eurocode 2	CSCT	Peiris-Ghali	Proposed Simple Method	Proposed General Method
(1)	(2)	(3)	(4)	(5)	(6)	(7)	(8)	(9)	(10)	(11)	(12)	(13)	(14)	(15)	(16)	(17)	(18)	(19)	(20)	(21)	(22)	(23)
75	1966	[23]	A1/M3	1370	1370	203	203	S	121	13.5	282	1.90	301.0	P	2.71	2.96	1.57	1.01	0.98	1.57	1.09	1.09
76	1966	[23]	A1/T1	1370	1370	203	203	S	124	13.3	432	1.00	254.0	P	1.43	3.04	1.29	1.01	0.91	1.29	1.10	1.10
77	1966	[23]	A1/T2	1370	1370	203	203	S	117	20.0	432	1.20	339.0	P	1.71	2.82	1.52	1.22	1.08	1.52	1.31	1.31
78	1966	[23]	A2/M1	1370	1370	203	203	S	124	33.6	255	1.00	401.0	F	1.43	0.87	1.28	1.17	1.08	1.34	1.28	1.31
79	1966	[23]	A2/M2	1370	1370	203	203	S	117	31.2	282	1.50	411.0	P	2.14	1.49	1.47	1.19	1.07	1.47	1.27	1.27
80	1966	[23]	A2/M3	1370	1370	203	203	S	121	30.9	282	1.90	422.0	P	2.71	1.96	1.45	1.07	0.98	1.45	1.15	1.15
81	1966	[23]	A2/T1	1370	1370	203	203	S	124	37.3	432	1.00	411.0	P	1.43	1.82	1.24	1.16	1.01	1.24	1.26	1.26
82	1966	[23]	A2/T2	1370	1370	203	203	S	124	39.3	432	1.70	431.0	P	2.43	3.01	1.27	1.00	0.88	1.27	1.09	1.09
83	1966	[23]	A3/M1	1370	1370	203	203	S	124	17.9	255	1.00	242.0	P	1.43	1.19	1.06	0.88	0.81	1.06	0.95	0.95
84	1966	[23]	A3/M2	1370	1370	203	203	S	102	18.3	282	1.70	330.0	P	2.43	1.92	1.86	1.36	1.25	1.86	1.40	1.40
85	1966	[23]	A3/M3	1370	1370	203	203	S	117	25.9	282	1.90	292.0	P	2.71	2.07	1.15	0.83	0.76	1.15	0.89	0.89
86	1966	[23]	A3/T1	1370	1370	203	203	S	121	19.6	432	1.00	322.0	P	1.43	2.45	1.39	1.18	1.03	1.39	1.27	1.27
87	1966	[23]	A3/T2	1370	1370	203	203	S	119	15.2	432	1.20	292.0	P	1.71	3.29	1.47	1.12	1.01	1.47	1.21	1.21
88	1966	[23]	A4/M1	1370	1370	203	203	S	114	36.4	255	1.10	254.0	P	1.57	0.85	0.87	0.81	0.74	0.91	0.86	0.88
89	1966	[23]	A4/M2	1370	1370	203	203	S	119	27.7	282	1.50	335.0	P	2.14	1.60	1.24	0.98	0.89	1.24	1.05	1.05
90	1966	[23]	A4/M3	1370	1370	203	203	S	117	30.6	322	1.90	531.0	P	2.71	2.32	1.92	1.43	1.29	1.92	1.53	1.53
91	1966	[23]	A4/T1	1370	1370	203	203	S	114	31.2	432	1.10	377.0	P	1.57	2.02	1.40	1.26	1.09	1.40	1.34	1.34
92	1966	[23]	A4/T2	1370	1370	203	203	S	117	27.8	432	1.20	394.0	P	1.71	2.39	1.50	1.27	1.11	1.50	1.36	1.36
93	1968	[24]	AN-1	2134	2134	254	254	S	111	18.7	403	1.54	334.0	P	2.20	2.52	1.42	1.13	1.10	1.42	1.12	1.12

No.	Year	Ref. [No.]	Slab ID	L_1 (mm)	L_2 (mm)	c_1 (mm)	c_2 (mm)	Column Shape	d (mm)	f'_c (MPa)	f_y (MPa)	ρ (%)	V_{exp} (kN)	Failure mode	ρ/ρ_{fs} Simplified Method	ρ/ρ_{fs} General Method	V_{exp}/V_{calc}					
																	ACI 318-14	Eurocode 2	CSCT	Peiris-Ghali	Proposed Simple Method	Proposed General Method
(1)	(2)	(3)	(4)	(5)	(6)	(7)	(8)	(9)	(10)	(11)	(12)	(13)	(14)	(15)	(16)	(17)	(18)	(19)	(20)	(21)	(22)	(23)
94	1968	[24]	BN-1	2134	2134	254	254	S	111	20.1	444	1.03	265.5	P	1.47	1.87	1.09	1.00	0.97	1.09	0.99	0.99
95	1970	[25]	P1	2900	2900	500	500	C	240	27.9	544	1.31	1662.0	P	1.87	3.36	1.44	1.32	1.09	1.44	1.17	1.17
96	1971	[10]	1	2134	2134	305	305	S	117	30.3	412	1.12	383.9	F	1.60	1.37	1.06	1.05	1.17	1.06	1.00	1.00
97	1971	[10]	2	2134	2134	406	203	R	117	26.3	412	1.12	351.4	S	1.60	1.92	1.04	1.01	1.12	1.04	1.13	1.13
98	1971	[10]	3	2134	2134	457	152	R	117	32.0	412	1.12	333.2	S	1.60	2.01	1.08	0.89	1.00	1.08	1.10	1.10
99	1971	[10]	4	2134	2134	495	114	R	117	31.0	412	1.12	330.5	S	1.60	2.30	1.24	0.90	1.00	1.24	1.18	1.18
100	1971	[10]	5	2134	2134	457	152	R	117	26.9	412	1.44	355.0	S	2.06	2.82	1.25	0.93	1.01	1.25	1.14	1.14
101	1971	[10]	6	2134	2134	457	152	R	117	22.7	412	1.12	335.8	F	1.60	2.39	1.29	1.01	1.12	1.29	1.24	1.24
102	1971	[10]	7	2134	2134	457	152	R	117	25.9	412	0.87	319.8	S	1.24	1.74	1.15	1.00	1.14	1.15	1.23	1.23
103	1971	[10]	8	2134	2134	495	114	R	121	26.1	414	0.81	314.5	S	1.16	1.89	1.23	0.95	1.09	1.23	1.27	1.27
104	1971	[10]	9	2134	2134	305	152	R	121	29.5	414	0.77	315.4	S	1.10	1.55	1.03	1.05	1.21	1.03	1.27	1.27
105	1971	[26]	A-S-000-0-0-2	737	737	102	102	S	46	35.1	359	1.15	65.4	P	1.65	1.18	1.23	1.18	0.95	1.23	1.18	1.18
106	1971	[26]	A-S-000-0-0-3	737	737	102	102	S	46	28.9	359	1.15	63.2	P	1.65	1.30	1.31	1.22	0.99	1.31	1.22	1.22
107	1971	[26]	A-S-000-0-0-4	737	737	102	102	S	46	28.9	359	1.15	61.0	P	1.65	1.30	1.26	1.18	0.95	1.26	1.17	1.17
108	1971	[26]	A-S-000-0-0-5	737	737	102	102	S	46	29.0	359	1.15	63.6	P	1.65	1.30	1.32	1.22	0.99	1.32	1.22	1.22
109	1971	[26]	B-S-000-0-0-1	737	737	102	102	S	46	31.4	368	2.53	88.2	P	3.61	2.84	1.75	1.38	1.08	1.75	1.28	1.28
110	1971	[26]	B-S-000-0-0-2	737	737	102	102	S	46	29.6	462	2.53	87.0	P	3.61	4.13	1.78	1.38	1.08	1.78	1.28	1.28
111	1971	[26]	H-0-a	737	737	102	102	S	46	30.3	374	1.15	67.1	P	1.65	1.35	1.36	1.27	1.03	1.36	1.27	1.27

No.	Year	Ref. [No.]	Slab ID	L_1 (mm)	L_2 (mm)	c_1 (mm)	c_2 (mm)	Column Shape	d (mm)	f'_c (MPa)	f_y (MPa)	ρ (%)	V_{exp} (kN)	Failure mode	ρ/ρ_{fs} Simplified Method	ρ/ρ_{fs} General Method	V_{exp}/V_{calc} ACI 318-14	Eurocode 2	CSCT	Peiris-Ghali	Proposed Simple Method	Proposed General Method
(1)	(2)	(3)	(4)	(5)	(6)	(7)	(8)	(9)	(10)	(11)	(12)	(13)	(14)	(15)	(16)	(17)	(18)	(19)	(20)	(21)	(22)	(23)
112	1971	[26]	H-0-b	737	737	102	102	S	46	29.0	440	1.15	81.4	P	1.65	1.77	1.68	1.57	1.25	1.68	1.56	1.56
113	1973	[27]	M	1400	1400	226	226	C	109	39.6	541	1.32	362.0	P	1.89	2.83	1.28	1.19	0.85	1.28	1.10	1.10
114	1977	[28]	DA6	1260	1260	100	100	S	80	30.0	550	1.79	183.0	P	2.56	5.91	1.74	1.20	1.11	1.74	1.40	1.40
115	1977	[28]	DA7	1260	1260	200	200	S	80	33.5	550	1.79	288.0	P	2.56	3.53	1.67	1.42	1.19	1.67	1.37	1.37
116	1977	[28]	DA10	1260	1260	240	240	S	80	32.0	550	1.79	281.0	P	2.56	3.22	1.46	1.29	1.08	1.46	1.19	1.19
117	1977	[28]	DA11	1260	1260	320	320	S	80	30.4	550	1.79	324.0	P	2.56	2.84	1.38	1.30	1.10	1.38	1.11	1.11
118	1977	[29]	P2	2750	2750	300	300	C	143	34.6	558	1.48	628.0	P	2.11	3.00	1.37	1.20	1.13	1.37	1.11	1.11
119	1979	[30]	P5	2750	2750	300	300	C	171	26.2	515	1.18	628.0	P	1.69	2.91	1.23	1.05	1.02	1.23	1.04	1.04
120	1980	[31]	S1	5820	4680	800	800	C	669	28.7	622	0.61	4915.0	P	0.87	5.51	0.75	0.93	0.77	0.75	1.23	1.20
121	1982	[32]	AB1	1900	1900	249	249	S	114	36.2	515	1.40	407.9	P	2.00	2.45	1.23	1.10	1.00	1.23	1.11	1.11
122	1982	[33]	S1	1800	1800	150	150	S	100	40.1	462	0.57	197.7	P	0.81	1.05	0.94	1.04	1.12	0.98	1.20	1.16
123	1982	[33]	S7	1800	1800	150	150	S	100	37.4	462	0.76	221.7	P	1.09	1.46	1.09	1.09	1.13	1.09	1.21	1.21
124	1982	[33]	S19	1800	1800	150	150	S	100	37.6	462	0.38	130.7	F	0.54	0.73	0.64	0.81	0.91	0.95	0.99	0.95
125	1984	[34]	0	1960	1960	210	210	C	113	23.1	420	0.83	280.0	P	1.18	1.55	1.29	1.24	1.01	1.29	1.19	1.19
126	1984	[34]	3	1960	1960	210	210	C	170	23.3	450	0.55	460.0	P	0.79	1.64	1.18	1.15	0.99	1.18	1.32	1.27
127	1986	[16]	I/1	2000	2000	200	200	S	77	25.8	500	1.20	194.0	P	1.72	1.89	1.34	1.26	1.17	1.34	1.21	1.21
128	1986	[16]	I/2	2000	2000	200	200	S	77	23.4	500	1.20	176.0	P	1.72	1.98	1.28	1.18	1.10	1.28	1.13	1.13
129	1986	[16]	I/3	2000	2000	200	200	S	77	27.4	500	0.92	194.0	P	1.31	1.40	1.30	1.35	1.26	1.30	1.29	1.29
130	1986	[16]	I/4	2000	2000	200	200	S	77	32.3	500	0.92	194.0	P	1.31	1.29	1.20	1.28	1.20	1.20	1.22	1.22

No.	Year	Ref. [No.]	Slab ID	L_1 (mm)	L_2 (mm)	c_1 (mm)	c_2 (mm)	Column Shape	d (mm)	f'_c (MPa)	f_y (MPa)	ρ (%)	V_{exp} (kN)	Failure mode	ρ/ρ_{fs} Simplified Method	ρ/ρ_{fs} General Method	V_{exp}/V_{calc} ACI 318-14	Eurocode 2	CSCT	Peiris-Ghali	Proposed Simple Method	Proposed General Method
(1)	(2)	(3)	(4)	(5)	(6)	(7)	(8)	(9)	(10)	(11)	(12)	(13)	(14)	(15)	(16)	(17)	(18)	(19)	(20)	(21)	(22)	(23)
131	1986	[16]	I/5	2000	2000	200	200	S	79	28.2	480	0.75	165.0	P	1.07	1.09	1.06	1.17	1.12	1.06	1.13	1.13
132	1986	[16]	I/6	2000	2000	200	200	S	79	21.9	480	0.75	165.0	P	1.07	1.24	1.20	1.27	1.21	1.20	1.23	1.23
133	1986	[16]	I/7	2000	2000	200	200	S	79	30.4	480	0.80	186.0	F	1.14	1.12	1.15	1.26	1.20	1.15	1.21	1.21
134	1986	[16]	II/1	3000	3000	250	250	C	200	34.9	530	0.98	825.0	P	1.40	2.81	1.24	1.07	1.07	1.24	1.18	1.18
135	1986	[16]	II/2	2000	2000	160	160	C	128	33.3	485	0.98	390.0	P	1.40	2.51	1.47	1.26	1.14	1.47	1.38	1.38
136	1986	[16]	II/3	2000	2000	160	160	C	128	34.3	485	0.98	365.0	P	1.40	2.47	1.35	1.16	1.15	1.35	1.28	1.28
137	1986	[16]	II/4	1000	1000	80	80	C	64	33.3	480	0.98	117.0	P	1.40	2.47	1.76	1.51	1.17	1.76	1.66	1.66
138	1986	[16]	II/5	1000	1000	80	80	C	64	34.3	480	0.98	105.0	P	1.40	2.44	1.56	1.34	1.11	1.56	1.47	1.47
139	1986	[16]	II/6	1000	1000	80	80	C	64	36.2	480	0.98	105.0	P	1.40	2.37	1.52	1.31	1.15	1.52	1.44	1.44
140	1986	[16]	III/1	1500	1500	150	150	C	95	23.2	494	0.83	197.0	P	1.19	2.23	1.42	1.29	1.06	1.42	1.32	1.32
141	1986	[16]	III/2	1500	1500	150	150	C	95	9.5	494	0.83	123.0	P	1.19	3.48	1.38	1.09	0.93	1.38	1.11	1.11
142	1986	[16]	III/3	1500	1500	150	150	C	95	37.8	494	0.83	214.0	P	1.19	1.75	1.21	1.19	0.98	1.21	1.21	1.21
143	1986	[16]	III/4	1500	1500	150	150	C	93	11.9	464	1.52	154.0	P	2.17	5.08	1.59	1.07	0.96	1.59	1.08	1.08
144	1986	[16]	III/5	1500	1500	150	150	C	93	26.8	464	1.52	214.0	P	2.17	3.39	1.48	1.13	0.95	1.48	1.15	1.15
145	1986	[16]	III/6	1500	1500	150	150	C	93	42.6	464	1.52	248.0	P	2.17	2.69	1.36	1.13	0.92	1.36	1.14	1.14
146	1986	[16]	V/1	1600	1600	54	54	C	118	34.3	628	0.80	170.0	P	1.14	5.14	1.11	0.80	0.79	1.11	1.16	1.16
147	1986	[16]	V/2	1600	1600	170	170	C	118	32.2	628	0.80	280.0	P	1.14	2.86	1.17	1.11	0.91	1.17	1.16	1.16
148	1986	[16]	V/3	1600	1600	110	110	C	118	32.4	628	0.80	265.0	P	1.14	3.73	1.37	1.15	1.01	1.37	1.39	1.39
149	1986	[16]	V/4	1600	1600	102	102	S	118	36.2	628	0.80	285.0	P	1.14	3.68	1.37	1.16	1.08	1.37	1.49	1.49

No.	Year	Ref. [No.]	Slab ID	L_1 (mm)	L_2 (mm)	c_1 (mm)	c_2 (mm)	Column Shape	d (mm)	f'_c (MPa)	f_y (MPa)	ρ (%)	V_{exp} (kN)	Failure mode	ρ/ρ_{fs} Simplified Method	ρ/ρ_{fs} General Method	V_{exp}/V_{calc} ACI 318-14	Eurocode 2	CSCT	Peiris-Ghali	Proposed Simple Method	Proposed General Method
(1)	(2)	(3)	(4)	(5)	(6)	(7)	(8)	(9)	(10)	(11)	(12)	(13)	(14)	(15)	(16)	(17)	(18)	(19)	(20)	(21)	(22)	(23)
150	1986	[16]	V/5	1600	1600	150	150	C	118	32.9	628	0.80	285.0	P	1.14	3.06	1.26	1.16	0.97	1.26	1.26	1.26
151	1987	[35]	1	700	700	100	100	S	41	40.0	530	0.42	36.4	FP	0.60	0.67	0.76	1.07	0.92	1.30	1.14	1.11
152	1987	[35]	2	700	700	100	100	S	41	40.0	530	0.55	49.1	P	0.79	0.89	1.02	1.32	1.10	1.33	1.33	1.30
153	1987	[35]	3	700	700	100	100	S	41	40.0	530	0.69	56.6	P	0.99	1.11	1.18	1.41	1.15	1.24	1.37	1.37
154	1987	[35]	4	700	700	100	100	S	41	40.0	530	0.82	56.2	P	1.17	1.32	1.17	1.32	1.06	1.17	1.29	1.29
155	1987	[35]	5	700	700	100	100	S	41	40.0	530	0.88	57.3	P	1.25	1.41	1.19	1.32	1.06	1.19	1.28	1.28
156	1987	[35]	6	700	700	100	100	S	41	40.0	530	1.04	65.6	P	1.48	1.67	1.37	1.43	1.14	1.37	1.39	1.39
157	1987	[35]	7	700	700	100	100	S	41	40.0	530	1.16	70.9	P	1.66	1.86	1.48	1.49	1.18	1.48	1.45	1.45
158	1987	[35]	8	700	700	100	100	S	41	40.0	530	1.29	71.7	P	1.84	2.07	1.49	1.45	1.15	1.49	1.41	1.41
159	1987	[35]	9	700	700	100	100	S	41	40.0	530	1.45	78.6	P	2.08	2.34	1.64	1.53	1.21	1.64	1.49	1.49
160	1987	[35]	10	700	700	100	100	S	41	40.0	530	0.52	43.6	P	0.74	0.83	0.91	1.20	1.00	1.26	1.22	1.20
161	1987	[35]	11	700	700	100	100	S	41	40.0	530	0.80	55.0	P	1.14	1.28	1.15	1.31	1.05	1.15	1.27	1.27
162	1987	[35]	12	700	700	100	100	S	41	40.0	530	1.12	67.1	P	1.59	1.79	1.40	1.43	1.13	1.40	1.39	1.39
163	1987	[35]	13	700	700	100	100	S	41	40.0	530	0.60	49.4	P	0.85	0.96	1.03	1.29	1.07	1.25	1.29	1.26
164	1987	[35]	14	700	700	100	100	S	41	40.0	530	0.69	52.5	P	0.99	1.11	1.09	1.31	1.07	1.15	1.27	1.27
165	1987	[35]	15	700	700	100	100	S	41	40.0	530	1.99	84.8	P	2.85	3.21	1.77	1.49	1.20	1.77	1.44	1.44
166	1987	[35]	1A	700	700	100	100	S	47	40.0	530	0.44	45.2	FP	0.62	0.81	0.79	1.06	0.90	1.17	1.15	1.10
167	1987	[35]	2A	700	700	100	100	S	47	40.0	530	0.69	66.2	P	0.99	1.29	1.15	1.33	1.08	1.15	1.34	1.34
168	1987	[35]	3A	700	700	100	100	S	47	40.0	530	1.29	89.7	P	1.85	2.40	1.56	1.46	1.17	1.56	1.47	1.47

No.	Year	Ref. [No.]	Slab ID	L_1 (mm)	L_2 (mm)	c_1 (mm)	c_2 (mm)	Column Shape	d (mm)	f'_c (MPa)	f_y (MPa)	ρ (%)	V_{exp} (kN)	Failure mode	ρ/ρ_{fs} Simplified Method	ρ/ρ_{fs} General Method	V_{exp}/V_{calc} ACI 318-14	Eurocode 2	CSCT	Peiris-Ghali	Proposed Simple Method	Proposed General Method
(1)	(2)	(3)	(4)	(5)	(6)	(7)	(8)	(9)	(10)	(11)	(12)	(13)	(14)	(15)	(16)	(17)	(18)	(19)	(20)	(21)	(22)	(23)
169	1987	[35]	4A	700	700	100	100	S	47	40.0	530	1.99	97.4	P	2.85	3.70	1.70	1.37	1.12	1.70	1.38	1.38
170	1987	[35]	1B	700	700	100	100	S	35	40.0	530	0.42	28.9	FP	0.61	0.58	0.73	1.06	0.92	1.36	1.08	1.09
171	1987	[35]	2B	700	700	100	100	S	35	40.0	530	0.69	37.6	P	0.99	0.95	0.94	1.18	0.96	1.11	1.10	1.11
172	1987	[35]	3B	700	700	100	100	S	35	40.0	530	1.29	56.7	P	1.84	1.77	1.42	1.44	1.14	1.42	1.34	1.34
173	1987	[35]	4B	700	700	100	100	S	35	40.0	530	1.99	72.5	P	2.84	2.73	1.82	1.59	1.27	1.82	1.49	1.49
174	1987	[35]	1C	700	700	100	100	S	54	40.0	530	0.42	62.7	FP	0.60	0.90	0.91	1.18	1.01	1.27	1.35	1.26
175	1987	[35]	2C	700	700	100	100	S	54	40.0	530	0.69	87.9	P	0.99	1.48	1.27	1.41	1.15	1.27	1.48	1.47
176	1987	[35]	3C	700	700	100	100	S	54	40.0	530	1.29	124.1	P	1.85	2.76	1.79	1.61	1.30	1.79	1.69	1.69
177	1987	[35]	4C	700	700	100	100	S	54	40.0	530	1.99	125.9	P	2.84	4.25	1.82	1.42	1.18	1.82	1.49	1.49
178	1988	[36]	S2.1	2540	2540	250	250	C	200	24.2	657	0.80	603.0	P	1.14	3.92	1.09	0.95	0.83	1.09	1.04	1.04
179	1988	[36]	S2.2	2540	2540	250	250	C	199	22.9	670	0.80	600.0	P	1.14	4.13	1.12	0.97	0.85	1.12	1.06	1.06
180	1988	[36]	S2.3	2540	2540	250	250	C	200	25.4	668	0.34	489.0	P	0.49	1.67	0.86	1.00	0.92	0.86	1.24	1.10
181	1988	[36]	S2.4	2540	2540	250	250	C	197	24.2	664	0.35	444.0	P	0.50	1.72	0.82	0.94	0.86	0.82	1.16	1.03
182	1988	[36]	S1.1	1270	1270	125	125	C	100	28.6	706	0.80	216.0	P	1.14	4.02	1.44	1.28	1.04	1.44	1.41	1.41
183	1988	[36]	S1.2	1270	1270	125	125	C	99	22.9	701	0.80	194.0	P	1.14	4.40	1.46	1.26	1.03	1.46	1.38	1.38
184	1988	[36]	S1.3	1270	1270	125	125	C	98	26.6	720	0.40	145.0	P	0.57	2.11	1.03	1.15	0.95	1.03	1.38	1.26
185	1988	[36]	S1.4	1270	1270	125	125	C	99	25.1	712	0.40	148.0	P	0.57	2.16	1.07	1.18	0.97	1.07	1.41	1.29
186	1990	[37]	5	483	483	102	102	C	38	13.1	550	2.04	33.0	P	2.91	7.16	1.39	1.01	0.76	1.39	0.86	0.86
187	1990	[37]	7	787	787	102	102	C	38	13.1	550	2.04	34.0	P	2.91	5.45	1.44	1.04	0.85	1.44	0.89	0.89

No.	Year	Ref. [No.]	Slab ID	L_1 (mm)	L_2 (mm)	c_1 (mm)	c_2 (mm)	Column Shape	d (mm)	f'_c (MPa)	f_y (MPa)	ρ (%)	V_{exp} (kN)	Failure mode	ρ/ρ_{fs} Simplified Method	ρ/ρ_{fs} General Method	V_{exp}/V_{calc} ACI 318-14	Eurocode 2	CSCT	Peiris-Ghali	Proposed Simple Method	Proposed General Method
(1)	(2)	(3)	(4)	(5)	(6)	(7)	(8)	(9)	(10)	(11)	(12)	(13)	(14)	(15)	(16)	(17)	(18)	(19)	(20)	(21)	(22)	(23)
188	1990	[37]	8	1219	1219	102	102	C	76	22.9	414	2.05	129.0	P	2.93	4.73	1.59	1.03	0.90	1.59	1.10	1.10
189	1990	[37]	9	787	787	102	102	C	76	21.5	414	2.05	136.0	P	2.93	5.52	1.73	1.11	0.92	1.73	1.18	1.18
190	1990	[37]	18	610	610	203	203	C	33	21.0	450	7.31	89.0	P	10.4 4	7.49	2.32	2.04	1.38	2.32	1.27	1.27
191	1990	[37]	26	991	991	203	203	C	73	49.5	450	5.01	323.0	P	7.16	6.85	1.88	1.73	0.98	1.88	1.35	1.35
192	1990	[38]	F3	914	914	102	102	C	83	38.0	531	1.75	149.0	P	2.50	5.73	1.27	0.91	0.73	1.27	1.01	1.01
193	1990	[38]	F4	1118	1118	102	102	C	83	38.0	531	1.75	129.0	P	2.50	5.24	1.10	0.79	0.65	1.10	0.87	0.87
194	1990	[38]	F5	1524	1524	102	102	C	83	38.0	531	1.75	139.0	P	2.50	4.80	1.18	0.85	0.74	1.18	0.94	0.94
195	1991	[39]	HS1	1700	1700	150	150	S	95	67.0	490	0.49	178.0	P	0.70	0.75	0.70	0.91	0.90	1.05	1.06	1.04
196	1991	[39]	HS2	1700	1700	150	150	S	95	70.0	490	0.84	249.0	P	1.20	1.26	0.96	1.04	0.97	0.96	1.15	1.15
197	1991	[39]	HS3	1700	1700	150	150	S	95	69.0	490	1.47	356.0	P	2.10	2.21	1.38	1.24	1.12	1.38	1.37	1.37
198	1991	[39]	HS4	1700	1700	150	150	S	90	66.0	490	2.37	418.0	P	3.39	3.47	1.79	1.46	1.25	1.79	1.50	1.50
199	1991	[39]	HS5	1700	1700	150	150	S	125	68.0	490	0.64	365.0	P	0.91	1.23	0.97	1.06	1.03	0.97	1.28	1.26
200	1991	[39]	HS6	1700	1700	150	150	S	120	70.0	490	0.94	489.0	P	1.34	1.73	1.35	1.33	1.24	1.35	1.56	1.56
201	1991	[39]	HS7	1700	1700	150	150	S	95	74.0	490	1.19	356.0	P	1.70	1.73	1.37	1.30	1.18	1.37	1.43	1.43
202	1991	[39]	HS8	1700	1700	150	150	S	120	69.0	490	1.11	436.0	P	1.59	2.05	1.22	1.13	1.05	1.22	1.32	1.32
203	1991	[39]	HS9	1700	1700	150	150	S	120	74.0	490	1.61	543.0	P	2.30	2.88	1.50	1.21	1.12	1.50	1.42	1.42
204	1991	[39]	HS10	1700	1700	150	150	S	120	80.0	490	2.33	645.0	P	3.33	4.00	1.78	1.31	1.15	1.78	1.45	1.45
205	1991	[39]	HS11	1700	1700	150	150	S	70	70.0	490	0.95	196.0	FP	1.36	1.06	1.14	1.30	1.19	1.14	1.31	1.31
206	1991	[39]	HS12	1700	1700	150	150	S	70	75.0	490	1.52	258.0	P	2.17	1.63	1.50	1.43	1.26	1.50	1.44	1.44

No.	Year	Ref. [No.]	Slab ID	L_1 (mm)	L_2 (mm)	c_1 (mm)	c_2 (mm)	Column Shape	d (mm)	f'_c (MPa)	f_y (MPa)	ρ (%)	V_{exp} (kN)	Failure mode	ρ/ρ_{fs} Simplified Method	ρ/ρ_{fs} General Method	V_{exp}/V_{calc}					
																	ACI 318-14	Eurocode 2	CSCT	Peiris-Ghali	Proposed Simple Method	Proposed General Method
(1)	(2)	(3)	(4)	(5)	(6)	(7)	(8)	(9)	(10)	(11)	(12)	(13)	(14)	(15)	(16)	(17)	(18)	(19)	(20)	(21)	(22)	(23)
207	1991	[39]	HS13	1700	1700	150	150	S	70	68.0	490	2.00	267.0	P	2.86	2.26	1.58	1.39	1.22	1.58	1.40	1.40
208	1991	[39]	HS14	1700	1700	220	220	S	95	72.0	490	1.47	498.0	P	2.10	1.64	1.49	1.48	1.31	1.49	1.47	1.47
209	1991	[39]	HS15	1700	1700	300	300	S	95	71.0	490	1.47	560.0	P	2.10	1.32	1.34	1.45	1.29	1.34	1.32	1.32
210	1991	[39]	NS1	1700	1700	150	150	S	95	42.0	490	1.47	320.0	P	2.10	2.84	1.59	1.32	1.20	1.59	1.45	1.45
211	1991	[39]	NS2	1700	1700	150	150	S	120	30.0	490	0.94	396.0	P	1.34	2.64	1.67	1.43	1.33	1.67	1.67	1.67
212	1992	[40]	P11FO	2750	2750	200	200	S	138	33.2	438	0.53	257.0	P	0.76	1.02	0.72	0.78	0.95	0.76	0.92	0.88
213	1992	[40]	P38FO	2750	2750	200	200	S	111	38.1	438	0.66	264.0	P	0.94	0.96	0.93	1.03	1.22	0.98	1.10	1.10
214	1992	[40]	P11S150	2750	2750	200	200	S	134	31.5	438	0.56	257.0	P	0.81	1.08	0.77	0.82	0.98	0.77	0.95	0.92
215	1992	[40]	P38S150	2750	2750	200	200	S	107	33.8	438	0.56	264.0	P	0.81	0.84	1.04	1.20	1.43	1.22	1.30	1.29
216	1992	[40]	P19S150	2750	2750	200	200	S	125	24.7	438	0.56	258.0	P	0.81	1.14	0.96	1.01	1.19	0.96	1.14	1.10
217	1992	[40]	P19S75	2750	2750	200	200	S	125	24.7	438	0.49	258.0	P	0.69	0.98	0.96	1.06	1.27	1.03	1.23	1.16
218	1992	[40]	P19S50	2750	2750	200	200	S	125	24.7	438	0.55	319.0	P	0.79	1.12	1.19	1.25	1.48	1.19	1.43	1.37
219	1992	[40]	P19RE	2750	2750	200	200	S	125	33.5	438	0.56	304.0	P	0.81	0.98	0.97	1.07	1.29	1.03	1.22	1.18
220	1992	[40]	P19RC	2750	2750	200	200	S	125	33.5	438	0.56	282.0	P	0.81	0.98	0.90	1.00	1.19	0.96	1.13	1.09
221	1992	[40]	P19RB	2750	2750	200	200	S	125	33.5	438	0.56	343.0	P	0.81	0.98	1.10	1.21	1.45	1.17	1.37	1.33
222	1993	[41]	FS-1	1800	1800	150	150	S	100	30.9	460	0.52	173.5	P	0.74	1.09	0.94	1.03	1.10	0.95	1.20	1.15
223	1993	[41]	FS-10	1800	1800	200	200	S	100	31.9	460	0.52	191.4	P	0.74	0.87	0.85	1.01	1.09	1.05	1.10	1.07
224	1993	[41]	FS-19	1800	1800	150	150	S	100	30.2	460	0.35	136.5	P	0.50	0.74	0.75	0.93	1.05	1.09	1.16	1.09
225	1993	[41]	FS-8	1800	1800	100	100	S	100	32.1	460	0.52	150.3	P	0.74	1.41	0.99	0.99	1.08	0.99	1.29	1.23

No.	Year	Ref. [No.]	Slab ID	L_1 (mm)	L_2 (mm)	c_1 (mm)	c_2 (mm)	Column Shape	d (mm)	f'_c (MPa)	f_y (MPa)	ρ (%)	V_{exp} (kN)	Failure mode	ρ/ρ_{fs} Simplified Method	ρ/ρ_{fs} General Method	V_{exp}/V_{calc} ACI 318-14	Eurocode 2	CSCT	Peiris-Ghali	Proposed Simple Method	Proposed General Method
(1)	(2)	(3)	(4)	(5)	(6)	(7)	(8)	(9)	(10)	(11)	(12)	(13)	(14)	(15)	(16)	(17)	(18)	(19)	(20)	(21)	(22)	(23)
226	1993	[42]	ND65-1-1	3000	3000	200	200	S	275	64.0	500	1.49	2050	P	2.13	4.21	1.47	1.15	1.23	1.47	1.43	1.43
227	1993	[42]	ND65-2-1	2600	2600	150	150	S	200	70.0	500	1.75	1200	P	2.50	4.53	1.54	1.08	1.20	1.54	1.44	1.44
228	1993	[42]	NG95-1-1	3000	3000	200	200	S	275	84.0	500	1.49	2250	P	2.13	3.67	1.54	1.15	1.23	1.54	1.43	1.43
229	1993	[42]	ND95-1-3	3000	3000	200	200	S	275	90.0	500	2.55	2400	P	3.64	6.07	1.65	1.09	1.08	1.65	1.26	1.26
230	1993	[42]	ND95-2-1	2600	2600	150	150	S	200	88.0	500	1.75	1100	P	2.50	4.04	1.41	0.92	1.01	1.41	1.22	1.22
231	1993	[42]	ND95-2-1D	2600	2600	150	150	S	200	87.0	500	1.75	1300	P	2.50	4.06	1.66	1.09	1.20	1.66	1.45	1.45
232	1993	[42]	ND95-2-3	2600	2600	150	150	S	200	90.0	500	2.62	1450	P	3.74	5.98	1.86	1.15	1.17	1.86	1.42	1.42
233	1993	[42]	ND95-2-3D	2600	2600	150	150	S	200	80.0	500	2.62	1250	P	3.74	6.34	1.60	1.03	1.05	1.60	1.27	1.27
234	1993	[42]	ND95-2-3D+	2600	2600	150	150	S	200	98.0	500	2.62	1450	P	3.74	5.73	1.86	1.15	1.13	1.86	1.38	1.38
235	1993	[42]	ND95-3-1	1500	1500	100	100	S	88	85.0	500	1.84	330.0	P	2.63	3.35	1.79	1.28	1.19	1.79	1.54	1.54
236	1993	[42]	ND115-1-1	3000	3000	200	200	S	275	112.0	500	1.49	2450	P	2.13	3.18	1.68	1.23	1.23	1.68	1.42	1.42
237	1993	[42]	ND115-2-1	2600	2600	150	150	S	200	119.0	500	1.75	1400	P	2.50	3.47	1.79	1.16	1.17	1.79	1.41	1.41
238	1993	[42]	ND115-2-3	2600	2600	150	150	S	200	108.0	500	2.62	1550	P	3.74	5.45	1.98	1.23	1.17	1.98	1.43	1.43
239	1994	[43]	A1	3180	3180	100	100	S	39	29.6	501	1.12	62.5	P	1.60	1.84	1.59	1.56	1.82	1.59	1.50	1.50
240	1994	[44]	SFO-1	1600	1600	64	64	S	70	33.4	420	1.40	90.0	P	2.00	3.33	1.26	0.89	0.80	1.26	1.13	1.13
241	1994	[44]	SFO-2	1600	1600	64	64	S	70	39.1	420	1.40	112.5	P	2.00	3.08	1.46	1.05	0.94	1.46	1.34	1.34
242	1994	[44]	SFO-3	1600	1600	64	64	S	70	31.1	420	1.40	81.0	P	2.00	3.46	1.18	0.82	0.74	1.18	1.04	1.04
243	1994	[44]	SFO-4	1600	1600	64	64	S	70	31.7	420	1.40	94.5	P	2.00	3.42	1.36	0.95	0.86	1.36	1.20	1.20
244	1995	[45]	I	600	600	100	100	C	55	39.0	448	0.51	65.0	P	0.73	0.98	0.99	1.20	0.79	1.21	1.23	1.17

No.	Year	Ref. [No.]	Slab ID	L_1 (mm)	L_2 (mm)	c_1 (mm)	c_2 (mm)	Column Shape	d (mm)	f'_c (MPa)	f_y (MPa)	ρ (%)	V_{exp} (kN)	Failure mode	ρ/ρ_{fs} Simplified Method	ρ/ρ_{fs} General Method	V_{exp}/V_{calc} ACI 318-14	Eurocode 2	CSCT	Peiris-Ghali	Proposed Simple Method	Proposed General Method
(1)	(2)	(3)	(4)	(5)	(6)	(7)	(8)	(9)	(10)	(11)	(12)	(13)	(14)	(15)	(16)	(17)	(18)	(19)	(20)	(21)	(22)	(23)
245	1995	[45]	II	600	600	100	100	C	55	50.3	448	0.51	61.0	P	0.73	0.86	0.82	1.04	0.68	1.13	1.06	1.03
246	1995	[45]	IV	600	600	100	100	C	55	39.0	448	0.51	60.0	P	0.73	0.98	0.91	1.11	0.73	1.12	1.14	1.08
247	1996	[46]	1	2400	2400	254	254	S	120	21.5	460	0.66	311.0	FP	0.94	1.63	1.12	1.18	1.21	1.12	1.20	1.19
248	1996	[47]	HSC0	2540	2540	250	250	C	200	90.3	643	0.80	965.0	P	1.14	1.96	1.03	0.98	0.97	1.03	1.07	1.07
249	1996	[47]	HSC1	2540	2540	250	250	C	200	91.3	627	0.80	1021	P	1.14	1.88	1.09	1.03	1.03	1.09	1.13	1.13
250	1996	[47]	HSC2	2540	2540	250	250	C	194	85.7	620	0.82	889.0	P	1.17	1.90	0.99	0.96	0.95	0.99	1.04	1.04
251	1996	[47]	HSC4	2540	2540	250	250	C	200	91.6	596	1.19	1041	P	1.70	2.59	1.11	0.92	0.89	1.11	1.01	1.01
252	1996	[47]	HSC6	2540	2540	250	250	C	201	108.8	633	0.60	960.0	P	0.86	1.31	1.01	1.06	1.04	1.01	1.12	1.10
253	1996	[47]	N/HSC8	2540	2540	250	250	C	198	94.9	631	0.80	944.0	P	1.14	1.84	1.02	0.97	0.95	1.02	1.05	1.05
254	1996	[47]	HSC9	2540	2540	250	250	C	202	84.1	634	0.33	565.0	FP	0.47	0.83	0.59	0.77	0.87	0.84	0.97	0.88
255	1996	[48]	N.H.Z.S.1.0	1900	1900	250	250	S	119	32.2	460	1.00	475.5	P	1.43	1.63	1.43	1.40	1.31	1.43	1.42	1.42
256	1996	[48]	N.N.Z.S.1.0	1900	1900	250	250	S	119	37.2	460	1.00	484.8	P	1.43	1.52	1.36	1.36	1.27	1.36	1.38	1.38
257	1996	[17]	1	1700	1700	150	150	C	98	88.2	550	0.60	224.0	F	0.86	1.00	0.89	0.99	0.99	0.90	1.05	1.02
258	1996	[17]	2	1700	1700	150	150	C	98	56.2	550	0.60	212.0	FP	0.86	1.25	0.94	1.09	1.06	0.94	1.15	1.12
259	1996	[17]	3	1700	1700	150	150	C	98	26.9	550	0.60	169.0	P	0.86	1.81	1.08	1.11	1.04	1.08	1.18	1.15
260	1996	[17]	4	1700	1700	150	150	C	98	58.7	550	0.60	233.0	F	0.86	1.22	1.01	1.18	1.15	1.01	1.25	1.22
261	1996	[17]	6	1700	1700	150	150	C	98	101.6	550	0.60	233.0	F	0.86	0.93	0.92	1.03	0.99	0.94	1.04	1.03
262	1996	[17]	12	1700	1700	150	150	C	98	60.4	550	1.30	319.0	P	1.86	2.61	1.36	1.24	1.12	1.36	1.28	1.28
263	1996	[17]	13	1700	1700	150	150	C	98	43.6	550	1.30	297.0	P	1.86	3.07	1.49	1.29	1.16	1.49	1.33	1.33

No.	Year	Ref. [No.]	Slab ID	L_1 (mm)	L_2 (mm)	c_1 (mm)	c_2 (mm)	Column Shape	d (mm)	f'_c (MPa)	f_y (MPa)	ρ (%)	V_{exp} (kN)	Failure mode	ρ/ρ_{fs} Simplified Method	ρ/ρ_{fs} General Method	V_{exp}/V_{calc} ACI 318-14	Eurocode 2	CSCT	Peiris-Ghali	Proposed Simple Method	Proposed General Method
(1)	(2)	(3)	(4)	(5)	(6)	(7)	(8)	(9)	(10)	(11)	(12)	(13)	(14)	(15)	(16)	(17)	(18)	(19)	(20)	(21)	(22)	(23)
264	1996	[17]	14	1700	1700	150	150	C	98	60.8	550	1.30	341.0	P	1.86	2.60	1.45	1.32	1.20	1.45	1.36	1.36
265	1996	[17]	16	1700	1700	150	150	C	98	98.4	550	1.30	362.0	FP	1.86	2.05	1.43	1.23	1.09	1.43	1.23	1.23
266	1996	[17]	21	1700	1700	150	150	C	98	41.9	650	1.30	286.0	P	1.86	4.03	1.46	1.26	1.03	1.46	1.29	1.29
267	1996	[17]	22	1700	1700	150	150	C	98	84.2	650	1.30	405.0	P	1.86	2.84	1.60	1.41	1.15	1.60	1.45	1.45
268	1996	[17]	23	1700	1700	150	150	C	100	56.4	650	0.90	341.0	P	1.29	2.45	1.46	1.48	1.23	1.46	1.53	1.53
269	1996	[17]	25	1700	1700	150	150	C	100	32.9	650	1.20	244.0	P	1.71	4.27	1.37	1.15	1.04	1.37	1.19	1.19
270	1996	[17]	26	1700	1700	150	150	C	100	37.6	650	1.20	294.0	P	1.71	4.00	1.54	1.33	1.10	1.54	1.38	1.38
271	1996	[17]	27	1700	1700	150	150	C	102	33.7	650	1.00	227.0	P	1.43	3.59	1.22	1.09	0.91	1.22	1.14	1.14
272	1997	[49]	L1	1770	1770	202	202	C	172	31.1	621	0.46	503.0	P	0.66	2.02	1.12	1.20	1.07	1.12	1.44	1.34
273	1997	[49]	L2	1770	1770	202	202	C	176	31.1	621	0.45	537.0	P	0.64	2.01	1.16	1.24	1.11	1.16	1.50	1.40
274	1997	[49]	L3	1770	1770	201	201	C	173	31.1	621	0.45	530.0	P	0.64	1.99	1.17	1.26	1.13	1.17	1.53	1.42
275	1997	[49]	L4	1970	1970	402	402	C	170	31.1	612	0.67	686.0	P	0.96	1.86	1.03	1.20	1.02	1.03	1.08	1.07
276	1997	[49]	L5	1970	1970	399	399	C	172	31.1	612	0.66	696.0	P	0.94	1.86	1.04	1.20	1.02	1.04	1.09	1.08
277	1997	[49]	L6	1970	1970	406	406	C	175	31.1	612	0.65	799.0	P	0.93	1.85	1.15	1.34	1.14	1.15	1.22	1.20
278	1997	[49]	L7	1970	1970	201	201	C	177	22.9	586	0.64	478.0	P	0.91	2.99	1.19	1.07	0.98	1.19	1.23	1.22
279	1997	[49]	L8	2470	2470	899	899	C	174	22.9	576	1.16	1111.0	P	1.66	2.13	1.09	1.19	1.06	1.09	0.83	0.83
280	1997	[49]	L9	2470	2470	897	897	C	172	22.9	576	1.17	1107.0	P	1.67	2.12	1.10	1.20	1.07	1.10	0.84	0.84
281	1997	[49]	L10	2470	2470	901	901	C	173	22.9	576	1.16	1079.0	P	1.66	2.12	1.06	1.16	1.04	1.06	0.81	0.81
282	1998	[50]	H.H.Z.S.1.0	1900	1900	250	250	S	119	67.2	460	1.00	511.5	P	1.43	1.13	1.07	1.18	1.12	1.07	1.19	1.19

No.	Year	Ref. [No.]	Slab ID	L_1 (mm)	L_2 (mm)	c_1 (mm)	c_2 (mm)	Column Shape	d (mm)	f'_c (MPa)	f_y (MPa)	ρ (%)	V_{exp} (kN)	Failure mode	ρ/ρ_{fs} Simplified Method	ρ/ρ_{fs} General Method	V_{exp}/V_{calc} ACI 318-14	Eurocode 2	CSCT	Peiris-Ghali	Proposed Simple Method	Proposed General Method
(1)	(2)	(3)	(4)	(5)	(6)	(7)	(8)	(9)	(10)	(11)	(12)	(13)	(14)	(15)	(16)	(17)	(18)	(19)	(20)	(21)	(22)	(23)
283	1998	[51]	S1-U	2300	2300	225	225	S	127	35.3	445	0.96	301.0	P	1.37	1.59	0.85	0.82	0.81	0.85	0.87	0.87
284	1998	[51]	S1-B	2300	2300	225	225	S	123	35.3	445	1.92	317.0	P	2.74	3.08	0.93	0.72	0.70	0.93	0.76	0.76
285	1998	[51]	S2-U	2300	2300	225	225	S	127	54.2	445	0.96	363.0	P	1.37	1.28	0.83	0.85	0.86	0.83	0.91	0.91
286	1998	[51]	S2-B	2300	2300	225	225	S	123	54.2	445	1.92	447.0	P	2.74	2.49	1.06	0.88	0.85	1.06	0.92	0.92
287	1998	[51]	S3-U	2300	2300	225	225	S	127	63.7	445	0.96	443.0	P	1.37	1.18	0.93	0.99	1.00	0.93	1.05	1.05
288	1998	[51]	S3-B	2300	2300	225	225	S	123	63.7	445	1.92	485.0	P	2.74	2.29	1.06	0.90	0.87	1.06	0.95	0.95
289	2000	[52]	9	2600	2600	250	250	S	150	26.9	500	0.52	408.0	P	0.74	1.30	0.98	1.09	1.16	0.98	1.24	1.18
290	2000	[52]	9a	2600	2600	250	250	S	150	21.0	500	0.52	360.0	P	0.74	1.47	0.98	1.04	1.10	0.98	1.18	1.13
291	2000	[53]	NU	2300	2300	225	225	S	110	30.0	444	1.11	306.0	P	1.58	1.75	1.14	1.05	1.03	1.14	1.08	1.08
292	2000	[53]	NB	2300	2300	225	225	S	110	30.0	444	2.15	349.0	P	3.07	3.39	1.30	0.99	0.94	1.30	0.98	0.98
293	2000	[54]	NSNW0.5P	1900	1900	250	250	S	120	37.8	450	0.49	310.2	F	0.70	0.73	0.85	1.08	1.10	1.26	1.17	1.16
294	2000	[55]	P100	925	925	201	201	S	99	39.3	488	0.97	330.0	P	1.39	2.25	1.33	1.34	1.03	1.33	1.38	1.38
295	2000	[55]	P150	1190	1190	201	201	S	150	39.3	464	0.90	582.7	P	1.29	2.40	1.33	1.23	1.04	1.33	1.41	1.41
296	2000	[55]	P200	1450	1450	201	201	S	201	39.3	464	0.83	902.9	P	1.19	2.55	1.34	1.18	1.08	1.34	1.46	1.46
297	2000	[55]	P300	1975	1975	201	201	S	300	39.3	468	0.76	1378.9	P	1.09	2.79	1.10	0.99	0.94	1.10	1.23	1.23
298	2000	[55]	P400	1975	1975	300	300	S	399	39.3	433	0.76	2224.0	P	1.09	3.22	0.95	0.94	0.83	0.95	1.24	1.24
299	2000	[55]	P500	1975	1975	300	300	S	500	39.3	433	0.76	2682.1	P	1.09	4.38	0.80	0.79	0.68	0.80	1.16	1.16
300	2000	[56]	1	2400	2400	120	120	S	93	60.9	695	1.50	270.0	P	2.14	4.63	1.31	1.09	1.08	1.31	1.26	1.26
301	2000	[56]	2	1700	1700	120	120	S	97	62.9	695	1.40	335.0	P	2.00	4.41	1.51	1.27	1.17	1.51	1.49	1.49

No.	Year	Ref. [No.]	Slab ID	L_1 (mm)	L_2 (mm)	c_1 (mm)	c_2 (mm)	Column Shape	d (mm)	f'_c (MPa)	f_y (MPa)	ρ (%)	V_{exp} (kN)	Failure mode	ρ/ρ_{fs} Simplified Method	ρ/ρ_{fs} General Method	V_{exp}/V_{calc} ACI 318-14	Eurocode 2	CSCT	Peiris-Ghali	Proposed Simple Method	Proposed General Method
(1)	(2)	(3)	(4)	(5)	(6)	(7)	(8)	(9)	(10)	(11)	(12)	(13)	(14)	(15)	(16)	(17)	(18)	(19)	(20)	(21)	(22)	(23)
302	2004	[11]	L1a	2280	1680	120	120	S	107	57.0	749	1.09	240.0	FP	1.56	4.20	0.98	0.86	0.79	0.98	1.04	1.04
303	2004	[11]	L1b	2280	1680	120	120	S	108	59.0	749	1.08	322.4	P	1.54	4.31	1.28	1.13	1.04	1.28	1.37	1.37
304	2004	[11]	L1c	2280	1680	120	120	S	107	59.0	749	1.09	318.0	P	1.56	4.32	1.28	1.13	1.04	1.28	1.36	1.36
305	2004	[11]	L2a	2280	1680	240	120	R	109	58.0	749	1.07	246.0	FP	1.53	3.84	0.77	0.76	0.67	0.77	0.95	0.95
306	2004	[11]	L2b	2280	1680	240	120	R	106	58.0	749	1.10	361.0	P	1.57	4.17	1.17	1.15	1.02	1.17	1.43	1.43
307	2004	[11]	L2c	2280	1680	240	120	R	107	57.0	749	1.09	330.8	P	1.56	4.11	1.07	1.05	0.93	1.07	1.31	1.31
308	2004	[11]	L3a	2280	1680	360	120	R	108	56.0	749	1.08	240.6	FP	1.54	3.66	0.77	0.68	0.60	0.77	0.86	0.86
309	2004	[11]	L3b	2280	1680	360	120	R	107	60.0	749	1.09	400.0	P	1.56	3.97	1.25	1.12	0.98	1.25	1.42	1.42
310	2004	[11]	L3c	2280	1680	360	120	R	106	54.0	749	1.10	357.6	P	1.57	3.96	1.19	1.05	0.92	1.19	1.33	1.33
311	2004	[11]	L4a	2280	1680	480	120	R	108	56.0	749	1.08	250.8	FP	1.54	3.49	0.76	0.64	0.57	0.76	0.83	0.83
312	2004	[11]	L4b	2280	1680	480	120	R	106	54.0	749	1.10	395.0	P	1.57	4.16	1.25	1.05	0.92	1.25	1.35	1.35
313	2004	[11]	L4c	2280	1680	480	120	R	107	56.0	749	1.09	404.0	P	1.56	3.66	1.24	1.05	0.92	1.24	1.35	1.35
314	2004	[11]	L5a	2280	1680	600	120	R	108	57.0	749	1.08	287.4	FP	1.54	3.35	0.81	0.67	0.60	0.81	0.88	0.88
315	2004	[11]	L5b	2280	1680	600	120	R	108	67.0	749	1.08	426.4	P	1.54	3.84	1.10	0.94	0.84	1.10	1.23	1.23
316	2004	[11]	L5c	2280	1680	600	120	R	109	63.0	749	1.07	446.4	P	1.53	3.28	1.18	0.99	0.89	1.18	1.30	1.30
317	2004	[3]	OC11	2200	2200	200	200	S	105	36.0	461	1.81	423.0	P	2.59	2.95	1.65	1.31	1.26	1.65	1.37	1.37
318	2004	[3]	OC13	2200	2200	600	200	R	107	35.8	461	1.71	568.0	P	2.44	2.61	1.57	1.27	1.21	1.57	1.46	1.46
319	2004	[3]	OC13-1.6	2200	2200	600	200	R	110	33.0	461	1.67	508.0	P	2.39	2.72	1.42	1.13	1.08	1.42	1.31	1.31
320	2004	[3]	OC13-0.63	2200	2200	600	200	R	111	39.7	461	1.65	455.0	P	2.36	2.48	1.15	0.94	0.90	1.15	1.09	1.09

No.	Year	Ref. [No.]	Slab ID	L_1 (mm)	L_2 (mm)	c_1 (mm)	c_2 (mm)	Column Shape	d (mm)	f'_c (MPa)	f_y (MPa)	ρ (%)	V_{exp} (kN)	Failure mode	ρ/ρ_{fs} Simplified Method	ρ/ρ_{fs} General Method	V_{exp}/V_{calc} ACI 318-14	Eurocode 2	CSCT	Peiris-Ghali	Proposed Simple Method	Proposed General Method
(1)	(2)	(3)	(4)	(5)	(6)	(7)	(8)	(9)	(10)	(11)	(12)	(13)	(14)	(15)	(16)	(17)	(18)	(19)	(20)	(21)	(22)	(23)
321	2004	[3]	OC15	2700	2200	1000	200	R	103	40.2	461	1.76	649.0	P	2.51	2.13	1.52	1.15	1.16	1.52	1.39	1.39
322	2006	[57]	NR1E0F0	1500	1500	200	200	S	100	20.5	507	0.73	188.0	P	1.04	1.94	1.04	1.03	0.90	1.04	1.06	1.06
323	2006	[57]	NR2E0F0	1500	1500	200	200	S	100	19.0	507	1.09	202.0	P	1.56	3.03	1.16	0.99	0.87	1.16	1.02	1.02
324	2006	[57]	HR1E0F0	1500	1500	200	200	S	100	70.3	471	1.49	331.0	P	2.14	1.93	0.99	0.95	0.82	0.99	0.97	0.97
325	2006	[57]	HR1E0F0r	1500	1500	200	200	S	100	71.3	471	1.49	371.0	P	2.14	1.92	1.11	1.06	0.91	1.11	1.09	1.09
326	2006	[57]	HR2E0F0	1500	1500	200	200	S	100	60.5	471	2.26	405.0	P	3.23	3.15	1.30	1.11	0.92	1.30	1.09	1.09
327	2006	[57]	HR2E0F0r	1500	1500	200	200	S	100	71.0	471	2.26	489.0	P	3.23	2.91	1.46	1.27	1.05	1.46	1.25	1.25
328	2008	[58]	1	2400	2400	250	250	S	124	36.2	488	1.54	483.0	P	2.20	2.71	1.30	1.11	1.13	1.30	1.14	1.14
329	2008	[58]	7	3400	3400	300	300	S	190	35.0	531	1.30	825.0	P	1.86	3.16	1.12	0.94	1.07	1.12	1.03	1.03
330	2008	[58]	10	4200	4200	350	350	S	260	31.4	524	1.00	1046	P	1.43	2.85	0.88	0.81	0.94	0.88	0.87	0.87
331	2008	[59]	30U	2300	2300	225	225	S	110	30.0	434	1.11	306.0	P	1.58	1.69	1.14	1.05	1.03	1.14	1.08	1.08
332	2008	[59]	30B	2300	2300	225	225	S	110	30.0	434	2.15	349.0	P	3.07	3.28	1.30	0.99	0.95	1.30	0.98	0.98
333	2008	[59]	35U	2300	2300	225	225	S	110	37.2	445	1.18	301.0	P	1.69	1.68	1.00	0.94	0.92	1.00	0.96	0.96
334	2008	[59]	35B	2300	2300	225	225	S	110	37.2	445	2.15	317.0	P	3.07	3.05	1.06	0.83	0.79	1.06	0.83	0.83
335	2008	[59]	55U	2300	2300	225	225	S	110	57.1	445	1.18	363.0	P	1.69	1.35	0.98	0.99	0.97	0.98	1.01	1.01
336	2008	[59]	55B	2300	2300	225	225	S	110	57.1	445	2.15	447.0	P	3.07	2.47	1.20	1.02	0.95	1.20	1.02	1.02
337	2008	[59]	65U	2300	2300	225	225	S	110	67.1	445	1.18	443.0	P	1.69	1.25	1.10	1.14	1.13	1.10	1.17	1.17
338	2008	[59]	65B	2300	2300	225	225	S	110	67.1	445	2.15	485.0	P	3.07	2.27	1.21	1.05	0.98	1.21	1.05	1.05
339	2009	[4]	PG-1	3000	3000	260	260	S	210	27.6	573	1.50	1023	P	2.14	5.52	1.48	1.08	1.17	1.48	1.25	1.25

No.	Year	Ref. [No.]	Slab ID	L_1 (mm)	L_2 (mm)	c_1 (mm)	c_2 (mm)	Column Shape	d (mm)	f'_c (MPa)	f_y (MPa)	ρ (%)	V_{exp} (kN)	Failure mode	ρ/ρ_{fs} Simplified Method	ρ/ρ_{fs} General Method	V_{exp}/V_{calc} ACI 318-14	Eurocode 2	CSCT	Peiris-Ghali	Proposed Simple Method	Proposed General Method
(1)	(2)	(3)	(4)	(5)	(6)	(7)	(8)	(9)	(10)	(11)	(12)	(13)	(14)	(15)	(16)	(17)	(18)	(19)	(20)	(21)	(22)	(23)
340	2009	[4]	PG-2b	3000	3000	260	260	S	210	40.6	552	0.25	440.0	F	0.36	0.72	0.52	0.74	0.96	0.92	1.02	0.91
341	2009	[4]	PG-3	6000	6000	520	520	S	456	32.4	520	0.33	2153.0	P	0.47	1.43	0.64	0.92	1.21	0.78	1.28	1.13
342	2009	[4]	PG-4	3000	3000	260	260	S	210	32.2	541	0.25	408.0	F	0.36	0.78	0.55	0.74	1.12	0.88	1.02	0.90
343	2009	[4]	PG-5	3000	3000	260	260	S	210	29.3	555	0.33	550.0	F	0.47	1.12	0.77	0.94	1.33	0.88	1.24	1.09
344	2009	[4]	PG-6	1500	1500	130	130	S	96	34.7	526	1.50	238.0	P	2.14	4.01	1.40	1.07	0.99	1.40	1.22	1.22
345	2009	[4]	PG-7	1500	1500	130	130	S	100	34.7	550	0.75	241.0	P	1.07	2.22	1.33	1.27	1.17	1.33	1.47	1.47
346	2009	[4]	PG-8	1500	1500	130	130	S	117	34.7	525	0.28	140.0	F	0.40	0.88	0.62	0.78	0.80	0.89	1.10	0.97
347	2009	[4]	PG-9	1500	1500	130	130	S	117	34.7	525	0.22	115.0	F	0.31	0.69	0.51	0.70	0.74	0.93	1.02	0.90
348	2009	[4]	PG-10	3000	3000	260	260	S	210	28.5	577	0.33	540.0	F	0.47	1.21	0.77	0.93	1.12	0.84	1.22	1.08
349	2009	[4]	PG-11	3000	3000	260	260	S	210	31.5	570	0.75	763.0	P	1.07	2.56	1.03	0.97	1.06	1.03	1.12	1.12
350	2010	[60]	S1	1500	1500	152	152	S	127	47.7	471	0.83	433.0	P	1.19	1.81	1.33	1.26	1.22	1.33	1.49	1.49
351	2010	[60]	S2	1500	1500	152	152	S	127	47.7	471	0.56	379.0	P	0.80	1.22	1.16	1.26	1.26	1.16	1.55	1.49
352	2012	[61]	A0	1050	1050	200	200	S	105	21.7	492	0.66	284.0	P	0.94	1.81	1.43	1.46	1.15	1.43	1.54	1.52
353	2012	[61]	B0	1350	1350	200	200	S	105	21.7	492	0.75	275.0	P	1.07	1.88	1.38	1.35	1.14	1.38	1.41	1.41
354	2012	[61]	C0	1650	1650	200	200	S	105	21.7	492	0.70	264.0	P	1.00	1.66	1.33	1.33	1.18	1.33	1.39	1.39
355	2012	[5]	S-1	1800	1800	249	249	S	117	28.4	433	0.43	252.2	F	0.61	0.68	0.83	1.06	1.05	1.29	1.16	1.14

No.	Year	Ref. [No.]	Slab ID	L_1 (mm)	L_2 (mm)	c_1 (mm)	c_2 (mm)	Column Shape	d (mm)	f'_c (MPa)	f_y (MPa)	ρ (%)	V_{exp} (kN)	Failure mode	ρ/ρ_{fs} Simplified Method	ρ/ρ_{fs} General Method	V_{exp}/V_{calc}					
																	ACI 318-14	Eurocode 2	CSCT	Peiris-Ghali	Proposed Simple Method	Proposed General Method
(1)	(2)	(3)	(4)	(5)	(6)	(7)	(8)	(9)	(10)	(11)	(12)	(13)	(14)	(15)	(16)	(17)	(18)	(19)	(20)	(21)	(22)	(23)
356	Authors' current slabs		S11-028	2200	2200	200	200	S	120	112.0	459	0.28	278.6	F	0.39	0.29	0.65	0.96	1.12	1.92	1.13	1.19
357			S11-050	2200	2200	200	200	S	117	112.0	459	0.50	393.6	F	0.72	0.51	0.95	1.16	1.21	1.58	1.22	1.29
358			S11-090	2200	2200	200	200	S	117	112.0	537	0.90	438.6	P	1.29	1.16	1.06	1.06	0.99	1.06	1.06	1.06
359			S11-139	2200	2200	200	200	S	114	112.0	501	1.39	453.6	P	1.99	1.58	1.14	0.99	0.89	1.14	0.98	0.98
360			S13-028	2200	2200	600	200	R	120	114.0	459	0.27	308.0	F	0.38	0.27	0.53	0.79	0.99	2.18	1.01	1.07
361			S13-050	2200	2200	600	200	R	117	114.0	537	0.50	418.0	F	0.72	0.63	0.74	0.91	0.97	1.44	1.04	1.06
362			S13-090	2200	2200	600	200	R	117	114.0	537	0.90	558.0	P	1.29	1.13	0.99	1.00	0.96	1.08	1.08	1.08
363			S13-143	2200	2200	600	200	R	114	114.0	501	1.43	718.0	P	2.04	1.57	1.32	1.14	1.05	1.32	1.23	1.23
364			S15-028	2700	2200	1000	200	R	117	97.0	459	0.27	321.3	F	0.38	0.25	0.49	0.68	0.97	2.42	0.97	1.04
365			S15-050	2700	2200	1000	200	R	117	97.0	537	0.50	456.3	F	0.71	0.58	0.70	0.79	0.95	1.59	1.00	1.04
366			S15-090	2700	2200	1000	200	R	117	97.0	537	0.90	656.3	P	1.29	1.06	1.00	0.93	1.00	1.28	1.12	1.12
367			S15-143	2700	2200	1000	200	R	114	97.0	501	1.43	775.3	P	2.04	1.47	1.22	0.98	0.99	1.22	1.17	1.17
																Minimum =	**0.49**	**0.64**	**0.57**	**0.75**	**0.73**	**0.76**
																Maximum =	**2.32**	**2.04**	**1.82**	**2.42**	**1.69**	**1.69**
																Average =	**1.26**	**1.14**	**1.04**	**1.31**	**1.21**	**1.20**
																COV=	**0.249**	**0.174**	**0.152**	**0.214**	**0.151**	**0.152**
																5th Percentile =	**0.75**	**0.80**	**0.76**	**0.90**	**0.91**	**0.89**

Note:
Unit conversion: 1 mm = 0.03937 in; 1 kN = 0.2248 kip; 1 MPa = 145.038 psi.)
Column (3) – [#] corresponds to the number of each reference given in the main paper and in pages A25 to A28
Column (9) – Column shapes: S = Square; R = Rectangular; C = Circular
Column (15) – Observed Failure Mode: F = Flexural Failure; P = Punching Failure
Column (16) – ρ_{fs} is taken to be 0.007 for the proposed Simplified Method as shown by Eq. (12b)
Column (17) – ρ_{fs} = proposed limiting reinforcement ratio, calculated using Eq. (12a)

NOTATIONS

Greek symbols

α_o = geometric coefficient for the strength of a slab calculated using yield line analysis ($V_{flex} = \alpha_o m$)
α_s = ACI 318's coefficient that accounts for the interior, edge and corner columns
β = ratio of long to short sides of the column
ψ = rotation of a slab
ρ = average reinforcement ratio
ρ_x = reinforcement ratio $100A_s/(L\times d)$ in the x-direction
ρ_y = reinforcement ratio $100A_s/(L\times d)$ in the y-direction
ρ_{fs} = limiting reinforcement ratio

Alphabetic symbols

A_s = Total cross-sectional area of flexural reinforcement within a slab length L
b_o = critical perimeter (used in ACI 318, CSCT, Peiris-Ghali, and authors' proposed Method)
b_1 = length of the longer side of critical perimeter b_o
b_2 = length of the shorter side of critical perimeter b_o
c_1 = length of the longer side of the column
c_2 = length of the shorter side of the column
d = average effective depth
d_g = maximum aggregate size
d_{go} = reference aggregate size (= 16 mm)
E_s = elastic modulus of steel reinforcement
f_c' = cylinder compressive strength of concrete
f_y = yield strength of flexural reinforcement
k = Eurocode 2's size effect factor
k_{CR} = column rectangularity factor (used in authors' proposed method)
k_{RR} = low reinforcement ratio factor (used in authors' proposed method)
k_{SZ} = size effect factor (used in the authors' proposed method)
L_1 = Length of the longer edge of the slab
L_2 = Length of the shorter edge of the slab
m = moment capacity per unit width
r = radius of a slab, taken as $0.2L$ where L is column-to-column span
r_s = radius of a slab used in CSCT, take as $0.22L$ where L is column-to-column span
u_1 = critical perimeter used in Eurocode 2 method
V = Shear load of a slab
V_c = punching shear strength of a slab
V_{calc} = calculated strength of a slab
V_{exp} = failure load (experimental) of a slab
V_{flex} = shear force that will cause flexural failure of the slab calculated using yield line analysis
V_{Rd} = punching shear strength (defined by Eurocode 2 and CSCT)

Acronyms

ACI = American Concrete Institute
COV = coefficient of variation
CSCT = critical shear crack theory
EC2 = Eurocode 2
HSC = high strength concrete
LVDT = linear variable differential transformers

REFERENCES (additional)

(Continued sequences from the main references)

1. Park, R. and W. L. Gamble (2000). Reinforced Concrete Slabs, John Wiley & Sons.
2. Elstner, R. C., and Hognestad, E. (1956). "Shearing Strength of Reinforced Concrete Slabs." ACI Journal, Proceedings V. 53(No. 1): pp. 29-58.
3. Swamy, R. N. ; Ali, S. A. R. (1982), "Punching Shear Behavior of Reinforced Slab-Column Connections Made with Steel Fiber Concrete." ACI Journal, Proceedings V. 79, No. 5, Sept.-Oct., pp. 392-406.
4. Regan, P. E. (1986). "Symmetrical Punching of Reinforced Concrete Slabs." Magazine of Concrete Research, V. 38, No. 136, Sept., pp. 115-128.
5. Ramdane, K. E. (1996). "Punching Shear of High Performance Concrete Slabs." Utilization of High Strength/High Performance Concrete, Laboratoire Central des Ponts et Chausées, Paris V. 3: pp. 1015-1026.
6. Guandalini, S., (2005) "Symmetric Punching in R/C Slabs," doctoral thesis, No. 3380, EPFL, Lausanne, Switzerland, 289 pp. (in French)
7. Graf, O. (1938). "Versuche über die Widerstandsfähigkeit von allseitig aufliegenden dicken Eisenbetonplatten unter Einzellasten." Deutscher Ausschuß für Eisenbeton Heft 88, Berlin: 26p.
8. Forssell, C. and E. Holmberg (1946). "Concentrated Loads on Concrete Slabs." Betong V. 31(No. 2): pp. 95-123.
9. Kinnunen, S. and H. Nylander (1960). "Punching of Concrete Slabs without Shear Reinforcement." Transaction No. 158, Royal Institute of Technology, Stockholm, Sweden: 112 pp.
10. Taylor, R. and B. Hayes (1965). " "Some Tests on the Effect of Edge Restraint on Punching Shear in Reinforced Concrete Slab," " Magazine of Concrete Research, V. 17, No. 50, Mar., pp. 39-44.
11. Base (1966). Data obtained from Databank collected by ACI committee 445C (2011) [Ref 12].
12. Corley, W. G. and N. M. Hawkins (1968). "Shearhead Reinforcement for Slabs." ACI Journal, Proceedings V. 65, No. 10, Oct., pp. 811-824.
13. Schaeidt, W. and M. Ladner (1970). "Berechnung von Flachdecken auf Durchstanzen," Schriftenreihe der Schweizerischen Zement-Industrie." Wildegg, Switzerland.
14. Roll, F., S. T. H. Zaidi, G. Sabnis and K. Chuang (1971). "Shear Resistance of Perforated Reinforced Concrete Slabs." ACI Publication, Cracking, Deflection and Ultimate Load of Concrete Slab Systems V. SP-30: pp. 77-101.
15. Ladner, M. (1973). "Einfluss der Maßstabsgröße bei Durchstanzversuchen - Ableitung eines begründeten Übertragungsgesetzes." Material und Technik No. 2: pp. 60-68.
16. Ladner, M., W. Schaeidt and S. Gut (1977). "Experimentelle Untersuchungen an Stahlbeton-Flachdecken." Eidgenössische Materialprüfungs- und Versuchsanstalt, Bericht Nr. 205, Dübendorf, Switzerland.
17. Marti, P., and Thürlimann, B. (1977). "“Fliessbedingung für Stahlbeton mit Berücksichtigung der Betonzugfestigkeit,." BuStb 72, H. 1(7-12).

18. Pralong, J., W. Brändli and B. Thürlimann (1979). "Durchstanzversuche an Stahlbetonund Spannbetonplatten." Institut für Baustatik und Konstruktion, ETH Zürich No. 7305-3: 89p.
19. Kinnunen, S., Nylander, H., and Tolf, P., "Plattjocklekens inverkan på betongplattors hållfasthet vid genomstansning. Försök med rektangulära plattor," Bulletin 137, Department of Structural Mechanics and Engineering, Royal Institute of Technology, Stockholm, Sweden, 1980, 73p. [Obtained from Ref [12]]
20. Mokhatar, A. (1982). Design of Stud Shear Reinforcement for Concrete Flat Plates. Department of Civil Engineering, University of Calgary. PhD Thesis.
21. Swamy, R. N. and S. A. R. Ali (1982). "Punching Shear Behavior of Reinforced Slab-Column Connections Made with Steel Fiber Concrete." ACI Journal, Proceedings V. 79, No. 5, Sept.-Oct., pp. 392-406.
22. Schaefers, U. (1984). "Konstruktion, Bemessung und Sicherheit gegen Durchstanzen von balkenlosen Stahlbetondecken im Bereich der Innenstützen." Deutscher Ausschuss für Stahlbeton Heft 357, Berlin: 72p.
23. Rankin, G. I. B. and A. E. Long (1987). "Predicting the Enhanced Punching Strength of Interior Slab-Column Connections." Institution of Civil Engineers, Proceedings V. 82(No. 3, Dec): pp 1165-1186.
24. Tolf, P. (1988). "Plattjocklekens inverkan på betongplattors hållfasthet vid genomestansning. Försök med cikulära plattor." Department of Structural Mechanics and Engineering, Royal Institute of Technology, Stockholm, Sweden Bulletin No. 146: 64 pp.
25. Gardner, N. J. (1990). "Relationship of the Punching Shear Capacity pf Reinforced Concrete Slabs with Concrete Strength." ACI STRUCTURAL JOURNAL V. 87(No. 1, Jan.-Feb): pp. 66-71.
26. Lovrovich, J. S. and D. I. Mclean (1990). "Punching Shear Behavior of Slabs Varying Span-Depth Ratios." ACI STRUCTURAL JOURNAL V. 87(No. 5, Sep.-Oct): pp. 507-511.
27. Marzouk, H. and A. Hussein (1991). "Punching Shear Analysis of Reinforced High-Strength Concrete Slabs." Canadian Journal of Civil Engineering, V. 18, No. 6, Dec., pp. 954-963.
28. Alexander, S. D. B. and S. H. Simmonds (1992b). "Test of Column-Flat Plate Connections." ACI STRUCTURAL JOURNAL 89(5): 495-502.
29. Theodorakopoulos, D. and N. Swamy (1993). "Contribution of Steel Fibers to the Strength Characteristics of Lightweight Concrete Slab-Column Connections Failing in Punching Shear." ACI STRUCTURAL JOURNAL Vol. 90(4): 342-355.
30. Tomaszewicz, A. (1993). "High Strength Concrete: SP2 - Plates and ShellsReport 2.3 Punching Shear Capacity of Reinforced Concrete Slabs." Report No. STF70 A93082, SINTEF Structures and Concrete, Trondheim, Norway, July, 36 pp.
31. Hallgren, M. (1996). Punching Shear Capacity of Reinforced High Strength Concrete Slabs. Doctoral Thesis, Royal Institute of Technology.
32. Shaaban, A. M. and H. Gesund (1994). "Punching Shear Strength of Steel Fiber Reinforced Concrete Flat Plates." ACI STRUCTURAL JOURNAL Vol. 91(3): 406-414.
33. Banthia, N., J. F. Trottier, P. Soroushian and Z. Bayasi (1992). "Fiber-Type Effects on the Performance of Steel Fiber Reinforced-Concrete - Discussion." Aci Materials Journal 89(1): 106-107.

34. Gardner, N. J. and X.-Y. Shao (1996). "Punching Shear of Continuous Flat Reinforced Concrete Slabs." ACI Structural Journal, V. 93, No. 2, Mar.-Apr., pp. 218-228.
35. Hallgren, M. (1996). Punching Shear Capacity of Reinforced High Strength Concrete Slabs. Department of Structural Engineering. Stockholm,Sweden, Royal Institute of Technology. Doctoral Thesis.
36. Marzouk, H., M. Emam and M. S. Hilal (1996). "Effect of High-Strength Concrete Columns on the Behavior of Slab-Column Connections." ACI STRUCTURAL JOURNAL V. 93(No. 5): pp. 1-8.
37. Sistonen, E., M. Lydman and S. Houinen (1997). Terasbetonilaatan Lavistyskapasiteetin Laskentakaavan Geometrinen Malli. Talonrakennustekniikan Laboratorio. Report 69 TKK/TRT.
38. Marzouk, H., M. Emam and M. S. Hilal (1998). "Effect of high-strength concrete slab on the behavior of slab-column connections." ACI STRUCTURAL JOURNAL 95(3): 227-237.
39. Ghannoum, C. M. (1998). Effect of high-strength concrete on the performance of slabcolumn specimens. Montreal, Canada, Mc Gill University. Masters Thesis: 85p.
40. Broms, C. E. (2000). "Elimination of Flat Plate Punching Failure Mode." ACI Structural Journal, V. 97, No. 1, Jan.-Feb., pp. 94-101.
41. McHarg, P. J. C., W. D.; Mitchell, D.; and Yoon, Y.-S. (2000a). "Improved Transmission of High-Strength Concrete Column Loads through Normal Strength Concrete Slabs." ACI STRUCTURAL JOURNAL 97(1): 149-157.
42. Osman, M., H. Marzouk and S. Helmy (2000). "Behavior of High-Strength Lightweight Concrete Slabs under Punching Loads." ACI Structural Journal, V. 97, No. 3, May-June 2000, pp. 492-498.
43. Li, K. K. L. (2000). Influence of Size on Punching Shear Strength of Concrete Slabs. Department of Civil Engineering and Applied Mechanics. Montreal,Quebec, McGill University. M. Eng.
44. Oliveira, D. R., G. S. Melo and P. E. Regan (2000). "Punching Strengths of Flat Plates with Vertical or Inclined Stirrups." ACI Structural Journal, V. 97, No. 3,May-June, pp. 485-491.
45. Ozden, S. and U. O. Ersoy, T. (2006). "Punching Shear Tests of Normal-and High-strength Concrete Flat Plates." Can. Ji. Civ. Eng, NRC Canada 33.
46. Birkle, G. and W. H. Dilger (2008). "Influence of slab thickness on punching shear strength." ACI STRUCTURAL JOURNAL 105(2): 180-188.
47. Lee, J.-H., Y.-S. Yoon, S.-H. Lee, W. D. Cook and D. Mitchell (2008). "Enhancing Performance of Slab-Column Connections." Journal of Structural Engineering, ASCE, V. 134, No. 3, Mar., pp. 448-45
48. Cheng, M.-Y. and G. J. Parra-Montesinos (2010a). "Evaluation of Steel Fiber Reinforcement for Punching Shear Resistance in Slab-Column Connections— Part I: Monotonically Increased Load." ACI STRUCTURAL JOURNAL Vol. 107(1): 101-109.
49. Nguyen-Minh, L., M. Rovňák and T. Tran-Quoc (2012). "Punching Shear Capacity of Interior SFRC Slab-Column Connections." Journal of Structural Engineering 138(5): 613-624.